Endocytosis of the damage-associated molecular pattern receptor PEPR1 is BAK1-dependent

Lucas Alves Neubus Claus[1,2], Fausto Andrés Ortiz-Morea[1,2,3,4], Shao-Li Yang[1,2], Shweta Yekondi[1,2], Xiangyu Xu[1,2], In-Cheol Yeo[3], Isabelle Vanhoutte[1,2], Nemanja Vukašinović[1,2], Qian Ma[1,2], Ive De Smet[1,2], Ping He[3], Libo Shan[3], and Eugenia Russinova[1,2,*]

[1]Department of Plant Biotechnology and Bioinformatics, Ghent University, 9052 Ghent, Belgium

[2]Center for Plant Systems Biology, VIB, 9052 Ghent, Belgium

[3]Department of Molecular, Cellular, and Developmental Biology, University of Michigan, Ann Arbor, Michigan 48109, USA

[4]Agricultural Engineering Program, University of the Amazon, Florencia 180002622, Colombia

Running title: BAK1 is required for PEPR1 internalization.

***Correspondence: Eugenia Russinova (eurus@psb.vib-ugent.be)**

ABSTRACT

After cellular damage caused by wounding or pathogens, *Arabidopsis thaliana* endogenous elicitor peptides (Peps) are released into the apoplast, enhancing innate immunity by directly binding to the membrane-localized leucine-rich repeat receptor kinase PEP RECEPTOR1 (PEPR1). Ligand binding induces PEPR1 heterodimerization with the co-receptor BRASSINOSTEROID INSENSITIVE1-ASSOCIATED KINASE1 (BAK1), followed by PEPR1 internalization, both essential for a subset of Pep1-induced responses. However, the role of BAK1 in Pep1-triggered PEPR1 endocytosis remains unclear. Here, we show that the ligand-induced PEPR1 endocytosis depends on its kinase activity and requires BAK1 C-terminal tail phosphorylation, which is equally indispensable for immune signaling and BAK1 internalization. Using a GFP insertional mutagenesis approach, we generated a partially functional GFP-tagged BAK1 to demonstrate that, following Pep1 elicitation, BAK1 and PEPR1 are endocytosed together with similar dynamics. Our findings identify the BAK1 function as a prerequisite for PEPR1 internalization.

Keywords: Arabidopsis, endogenous peptides, endocytosis, BAK1

38 **INTRODUCTION**

39

40 Damage-associated molecular patterns (DAMPs) are endogenous elicitor molecules released
41 into the apoplast after cell damage to trigger immune responses. An example of DAMPs in
42 plants is endogenous plant elicitor peptides (Peps) (Hou et al., 2019). Peps are 23-amino-acid
43 peptides that mature from a conserved C-terminal region of larger precursor proteins,
44 designated PROPEPs (Yamaguchi and Huffaker, 2011), which belong to a family of eight
45 members (PROPEP1 to PROPEP8) in *Arabidopsis thaliana* (Arabidopsis). Peps are recognized
46 by two homologous pattern recognition receptors (PRRs), the leucine-rich repeat (LRR)
47 receptor kinases (RKs) PEP RECEPTOR1 (PEPR1) and PEPR2 (Krol et al., 2010; Yamaguchi
48 et al., 2010; Bartels et al., 2013). The Pep-PEPR ligand-receptor pair is also present in other
49 dicots, such as *Solanaceae* and *Fabaceae* (Trivilin et al., 2014; Bartels and Boller, 2015), as
50 well as monocots, such as *Zea mays* (maize) (Huffaker et al., 2011, 2013).

51 Upon Pep1 binding, PEPR1 associates with the LRR co-receptor, BRASSINOSTEROID-
52 INSENSITIVE1 (BRI1)-ASSOCIATED RECEPTOR KINASE1 (BAK1)/SOMATIC
53 EMBRYOGENESIS RECEPTOR KINASE (SERK3), hereafter referred to as BAK1 (Tang et
54 al., 2015; Yamada et al., 2016). BAK1 is a promiscuous protein that regulates multiple signaling
55 pathways controlling growth, cell death, and innate immunity by forming ligand-dependent
56 complexes with several plasma membrane (PM)-localized RKs (Schulze et al., 2010;
57 Schwessinger et al., 2011). This raises the question of how BAK1 distinguishes between
58 different signaling pathways and responds accordingly. BAK1 has been shown to discriminate
59 between immune and brassinosteroid (BR) hormone responses in a phosphorylation-dependent
60 manner (Perraki et al., 2018). Accordingly, the *bak1-5* mutant allele, which carries a single
61 amino acid substitution (Cys to Tyr at position 408) in the kinase domain, leading to reduced
62 phosphorylation, is severely impaired in immune responses, but not in responses to BRs or cell
63 death (Schwessinger et al., 2011).

64 After perceiving Pep1, PEPR1 undergoes clathrin-mediated endocytosis (CME)
65 (Mbengue et al., 2016; Ortiz-Morea et al., 2016), an evolutionarily conserved process that is
66 essential for immunity and development in plants (Claus et al., 2018). CME regulates the
67 abundance of signaling components in the PM that are important for nutrient uptake (Takano
68 et al., 2010; Wang et al., 2017; Dubeaux et al., 2018), hormone signaling (Irani et al., 2012),
69 pathogen recognition, and stress responses (Krol et al., 2010; Choi et al., 2014). Previously,
70 PEPR1 was found to be internalized from the PM to the late endosome/multivesicular bodies
71 (LE/MVBs), bypassing the trans-Golgi network/early endosomes (TGN/EEs), from where it is

72 targeted to the vacuole for degradation (Ortiz-Morea et al, 2016). PEPR1 shares an
73 endomembrane trafficking pathway with the PRRs recognizing the microbe-associated
74 molecular patterns (MAMPs), such as FLAGELLIN-SENSING2 (FLS2) and EF-TU
75 RECEPTOR (EFR) (Robatzek et al., 2006; Mbengue et al., 2016), but differs from the well-
76 studied BR receptor BRI1, which is internalized from the PM to TGN/EE, where it can be
77 recycled back to the PM or targeted to the vacuole for degradation (Irani et al., 2012).

78 Endocytosis is often considered as a mechanism for removing receptors from the PM to
79 avoid continuous signaling that is potentially harmful to cells (Sigismund et al., 2012; Jaillais
80 and Vert, 2016). For example, in plants, blocking BRI1 endocytosis at the PM results in
81 constitutive BR responses, indicating that endocytosis attenuates BR signaling (Irani et al.,
82 2012; Martins et al., 2015; Zhou et al., 2018; Liu et al., 2020). However, disruption of PRR
83 endocytosis affects negatively plant defense responses (Ortiz-Morea et al., 2016; Mbengue et
84 al., 2016; Ekanayake et al., 2021).

85 Although considerable progress has been made in understanding the mechanisms of plant
86 receptor endocytosis, they remain poorly understood compared to their mammalian
87 counterparts. Post-translational modifications (PTMs), such as phosphorylation and
88 ubiquitination, are important regulators of FLS2 and BRI1 receptor endocytosis (Robatzek et
89 al., 2006; Mbengue et al., 2016; Lu et al., 2011; Martins et al., 2015; Zhou et al., 2018; Ma et
90 al., 2020). How the co-receptor BAK1 regulates endocytosis of the major receptors is still
91 unclear, because studies of BAK1 endocytosis in Arabidopsis have been hampered by the
92 observation that the C-terminally tagged BAK1 is not fully functional (Ntoukakis et al., 2011;
93 Lozano-Durán et al., 2013).

94 Here we sought to investigate the role of BAK1 in PEPR1 endocytosis. We found that, in
95 contrast to BRI1, the Pep1-induced endocytosis of PEPR1 requires BAK1 phosphorylation in
96 the C-terminal tail domain that is essential for both DAMP signaling and BAK1 endocytosis.
97 We further showed that the kinase activity of PEPR1 is necessary for its internalization and that
98 PEPR1 but not BAK1 was able to trans-phosphorylate *in vitro*. A GFP insertional mutagenesis
99 approach was used to generate a partially functional GFP-tagged BAK1, showing that following
100 Pep1 application BAK1 and PEPR1 are endocytosed together.

101

102 **RESULTS**

103

104 **Pep1-triggered responses are impaired by the C-terminal GFP-tagged BAK1 fusion**
105 **protein**

106 Arabidopsis plants expressing C-terminally tagged BAK1 variants exhibit impaired immune
107 responses to flg22 and elf18, but largely retain normal responses to exogenous BRs (Ntoukakis
108 et al., 2011; Lozano-Durán et al., 2013). Therefore, we tested whether the C-terminal tag of
109 BAK1 also interferes with responses to exogenous Pep1. To this end, we generated transgenic
110 Arabidopsis plants expressing native promoter-driven BAK1-GFP in the *bak1-4* mutant and
111 analyzed two independent transgenic lines (Supplemental Figure 1A-1E). BAK1-GFP
112 complemented the growth phenotype of *bak1-4* and remained functional in BR responses
113 (Supplemental Figure 1A-1E), although it caused slight BR hypersensitivity, possibly due to
114 increased expression levels (Supplemental Figure 1B and 1C). As previously described,
115 exogenous Pep1 inhibited wild-type root growth in a dose-dependent manner, whereas *bak1-4*
116 was hypersensitive to Pep1 (Figure 1A and 1B) due to sensitized PEPR signaling towards cell
117 death (Yamada et al., 2016). However, BAK1-GFP/*bak1-4* plants were insensitive to the Pep1-
118 induced root growth arrest, both MAPK activation and reactive oxygen species (ROS) burst
119 triggered by Pep1 were lower than in the wild-type, although the MAPK activation was less
120 affected (Figure 1C and 1D). Our findings indicate that, in addition to flg22 and elf18, the C-
121 terminal tag of BAK1 impairs Pep1 responses.
122
123 **BAK1 differentially regulates endocytosis of PEPR1 and BRI1**
124 Since exogenous Pep1 induces PEPR1 endocytosis (Ortiz-Morea et al., 2016), we tested
125 whether the C-terminally GFP-tagged BAK1 affects endocytosis of the Pep1-bound PEPR1 by
126 monitoring the internalization of the bioactive TAMRA-labelled Pep1 (TAMRA-Pep1) (Ortiz-
127 Morea et al., 2016) in BAK1-GFP/*bak1-4* plants (Figure 2A and 2B). As a control, we
128 quantified endocytosis of the fluorescent Alexa Fluor 647-castasterone (AFCS), a bioactive
129 fluorescently labelled BR analogue that is internalized together with BRI1 (Irani et al., 2012)
130 (Figure 2C and 2D). In contrast to the wild-type, TAMRA-Pep1 internalization was strongly
131 inhibited in BAK1-GFP/*bak1-4* plants, with few TAMRA-Pep1 puncta appearing inside the
132 cell and a strong signal remaining in the PM (Figure 2A and B). However, TAMRA-Pep1
133 internalization in the *bak1-4* mutant was not significantly different from that of the wild-type
134 at the analyzed time point (40 min chase) (Figure 2A and 2B). Consistently, exogenous Pep1-
135 induced PEPR1-GFP internalization in *bak1-4* and *pepr1pepr2* at 40 min (Supplemental Figure
136 2A) resembled TAMRA-Pep1 (Figure 2A and 2B) in both mutants but was partially inhibited
137 at later time points (60-120 min) in *bak1-4*. The AFCS uptake in BAK1-GFP/*bak1-4* and *bak1-*
138 *4* plants was comparable to or slightly higher than that of the wild-type (Figure 2C and 2D),

139 suggesting that C-terminally tagged BAK1 affects Pep1-PEPR1, but not AFCS-BRI1
140 endocytosis.
141 To confirm the importance of BAK1 for PEPR1 endocytosis, we examined the
142 internalization of PEPR1-GFP and TAMRA-Pep1 in different *serk* mutant combinations after
143 40 min chase (Supplemental Figure 2B-2E). TAMRA-Pep1 internalization was unaffected in
144 the *bak1-3serk4-1* double and the *serk1-1serk2-1serk4-1* triple mutant but was strongly
145 inhibited in the *serk1-1bak1-4* double mutant and the *serk1-1serk2-1bak1-4* triple mutant
146 (Supplemental Figure 2B-2E). These findings suggest that BAK1 and SERK1 redundantly
147 regulate PEPR1 endocytosis.
148 Taken together, our results show that the C-terminally tagged BAK1 impairs ligand-induced
149 endocytosis of PEPR1 but not BRI1, implying that BAK1 differentially regulates the
150 internalization of BR-bound BRI1 and Pep1-bound PEPR1.
151
152 **The C-terminal phosphorylation of BAK1 is essential for PEPR1 endocytosis and**
153 **signaling**
154 Given that the function of Arabidopsis BAK1 in immunity, but not in BR-regulated growth, is
155 regulated by conserved phosphorylation sites (S602, T603, S604 and S612) in its C-terminal
156 tail, and the C-terminal GFP-tagged BAK1 loses phosphorylation at one of these residues
157 (S612) (Perraki et al., 2018), we hypothesized that these phosphorylation sites might be
158 essential for Pep1-PEPR1 endocytosis and signaling. To test this hypothesis, we compared
159 TAMRA-Pep1 endocytosis in the phosphorylation-deficient $BAK1^{S612A}$ and
160 $BAK1^{S602AT603AS604A}$ (hereafter $BAK1^{AAA}$) mutants with that of the wild-type. Similar to BAK1-
161 GFP, both $BAK1^{S612A}$ and $BAK1^{AAA}$ showed a strong reduction in TAMRA-Pep1 uptake, with
162 the effect more pronounced in $BAK1^{S612A}$ (Figure 3A and 3B). Likewise, endocytosis of
163 PEPR1-GFP was impaired in both phosphorylation-deficient BAK1 variants expressed in the
164 *bak1-4* background, with a stronger effect observed in the $BAK1^{S612A}$ mutant (Figure 3C and
165 3D).
166 Since PEPR1-Pep1 endocytosis was impaired in the $BAK1^{S612A}$ and $BAK1^{AAA}$ mutants,
167 we suspected that the Pep1-induced signaling would also be disturbed. To test this hypothesis,
168 we performed root growth, MAPK activation and ROS burst assays after Pep1 treatment (Figure
169 4A-4D; Supplemental Figure 3). Similar to BAK1-GFP/*bak1-4*, $BAK1^{S612A}$/*bak1-4* and
170 $BAK1^{AAA}$/*bak1-4* plants were strongly insensitive to Pep1 treatment (Figure 4A and 4B) and
171 both MAPK activation (Figure 4C) and ROS burst were reduced compared to the wild-type
172 (Figure 4D). To further confirm that BAK1 phosphorylation is crucial for Pep1-induced

173 endocytosis, we analyzed the *bak1-5* mutant, which carries the C408Y point mutation,
174 responsible for the BAK1 hypoactivity (Schwessinger et al., 2011). *bak1-5* resembled BAK1-
175 GFP/*bak1-4*, BAK1^{S612A}/*bak1-4*, and BAK1^{AAA}/*bak1-4* plants in that it was less responsive to
176 exogenous Pep1 in the root growth inhibition assay (Supplemental Figure 4A and 4B),
177 consistent with previous findings for the MAMPs flg22 and elf18 (Schwessinger et al., 2011).
178 Additionally, Pep1-PEPR1 endocytosis was impaired in *bak1-5* mutant (Supplemental Figure
179 4C and 4D). Taken together, our results indicate that C-terminal BAK1 phosphorylation, which
180 is indispensable for flg22, elf18, and Pep1 signaling, is also a prerequisite for Pep1-induced
181 PEPR1 endocytosis.
182
183 **BAK1 does not trans-phosphorylate PEPR1 *in vitro***
184 To investigate the phosphorylation relationship between PEPR1 and BAK1, we performed an
185 *in vitro* kinase assay (Figure 5) using bacterially produced cytoplasmic domains (CDs) of
186 BAK1^{S612A}, BAK1^{AAA}, BAK1-5, BAK1, and PEPR1, along with their respective kinase-dead
187 mutant (Km) versions, PEPR1-Km (K855E) and BAK1-Km (D416N). These proteins were
188 tagged with either glutathione S-transferase (GST) or His6-maltose-binding protein (MBP).
189 Consistent with previous observations, BAK1-CD exhibited strong autophosphorylation
190 activity, whereas the BAK1-Km-CD was completely inactive (Wang et al., 2008). PEPR1-CD
191 also displayed autophosphorylation, though weaker than BAK1, while PEPR1-Km-CD was
192 inactive. Similarly, BAK1^{S612A} retained kinase activity, whereas BAK1^{AAA} and BAK1-5 were
193 hypoactive (Schwessinger et al., 2011; Perraki et al., 2018). Surprisingly, PEPR1-CD trans-
194 phosphorylated BAK1-Km-CD, whereas the BAK1-CD did not trans-phosphorylate PEPR1-
195 Km-CD. To confirm BAK1-CD trans-phosphorylation capacity, we tested its ability to
196 phosphorylate the bacterially produced GST-BOTRYTIS-INDUCED KINASE1 (BIK1)-Km
197 protein (Lu et al., 2010). As expected, BAK1 strongly trans-phosphorylated BIK1-Km protein
198 (Supplemental Figure 5). Additionally, in the presence of PEPR1-CD, phosphorylation of
199 BAK1-CD, BAK1-5-CD and BAK1^{S612A}-CD was reduced compared to when PEPR1-Km-CD
200 was used (Figure 5). However, this reduction did not occur for BAK1^{AAA}, whose
201 phosphorylation remained unchanged regardless of whether PEPR1-CD or PEPR1-Km-CD was
202 present. In summary, PEPR1 trans-phosphorylated BAK1 *in vitro*, but BAK1 had no detectable
203 phosphorylation activity toward PEPR1. The *in vitro* auto- and trans-phosphorylation sites in
204 BAK1 and PEPR1 were identified through mass spectrometry (MS) analysis (Supplemental
205 Dataset 1). As previously reported, BAK1 autophosphorylates at multiple residues (Wang et
206 al., 2008). In the kinase domain of PEPR1, 19 autophosphorylation sites were identified,

207 including S814, S848, S861, and T986, which were also found *in vivo* (Willems et al., 2024)
208 (Supplemental Dataset 2). Notably, PEPR1 phosphorylated BAK1 *in vitro* at six residues (S290,
209 T324, T446, T449, T450 and T455), four of which (T446, T449, T450 and T455) are located
210 in the BAK1 activation loop. To validate the phosphorylation relationship between PEPR1 and
211 BAK1 *in vivo*, we co-expressed PEPR1-Km-GFP with BAK1-mCherry in the *Nicotiana*
212 *benthamiana* leaf epidermis with or without Pep1 (500 nM) treatment for 15 min, and
213 performed MS-based phospho-analysis (Supplemental Dataset 2). Although, co-expression
214 with BAK1 did not change the phosphorylation state of PEPR1-Km-GFP, it increased the
215 phosphorylation of PEPR1 at T896 when Pep1 was added. Altogether, our data suggest that the
216 phosphorylation relationship between BAK1 and PERP1 *in vivo* is complex and it might be
217 influenced by additional factors involved in complex activation.
218
219 **Pep1 endocytosis requires kinase-active PEPR1**
220 Endocytosis of membrane proteins depends on their prior phosphorylation (Wang et al., 2017;
221 Zhou et al., 2018). To investigate whether phosphorylation of PEPR1 after ligand binding is
222 required for its internalization, we generated transgenic plants expressing a kinase-dead PEPR1-
223 GFP (PEPR1-Km-GFP) in the *pepr1pepr2* double mutant (Supplemental Figure 6A). As
224 previously reported (Ortiz-Morea et al., 2016), without elicitation, PEPR1-GFP localized
225 mainly to the PM, with a few puncta inside the cell. Pep1 treatment triggered its internalization,
226 with an endocytosis peak after 40 min. However, endocytosis of PEPR1-Km-GFP after Pep1
227 application was decreased, and the delay was most apparent 90-120 min after elicitation, when
228 the fluorescence signal almost disappeared, although the PM signal remained stronger.
229 Interestingly, without exogenous Pep1, PEPR1-Km-GFP was observed in intracellular puncta,
230 possibly indicating either endocytosis of PEPR1-Km-GFP without ligand binding or increase
231 of its *de novo* production and exocytosis (Supplemental Figure 6A). To further investigate, we
232 treated PEPR1-GFP and PEPR1-Km-GFP plants with Brefeldin A (BFA), an inhibitor of
233 endosomal trafficking, that induces aggregation of the *trans*-Golgi network/early endosome
234 (TGN/EE) compartments, forming BFA bodies (Geldner et al., 2003) (Supplemental Figure
235 6B). Without Pep1 elicitation, PEPR1-GFP was only weakly present in the BFA bodies, but
236 after Pep1 application, PEPR1-GFP puncta were excluded from the BFA bodies and localized
237 to the periphery of the TGN/EE aggregates. Notably, under both Pep1-treated or mock
238 conditions, the PEPR1-Km-GFP labelling of the BFA bodies was strong, suggesting that the
239 BFA bodies accumulate both internalized and secreted PEPR1-Km-GFP (Supplemental Figure
240 6B).

241 Cycloheximide (CHX), which blocks *de novo* protein synthesis, is routinely used to avoid
242 the interference from secreted proteins when analyzing endocytosis or recycling (Liu et al.,
243 2020). Unexpectedly, CHX blocked PEPR1 internalization (Supplemental Figure 7A) and
244 disturbed the Pep1-triggered MAPK activation (Supplemental Figure 7B). To overcome this
245 limitation, we used TAMRA-Pep1, which allows the tracking of PEPR1 internalization from
246 the PM. In contrast to PEPR1-GFP, the endocytosis of PEPR1-Km-GFP was reduced after
247 TAMRA-Pep1 application (Supplemental Figure 6C). After BFA treatment, TAMRA-Pep1
248 does not label the BFA bodies in plants expressing either PEPR1-GFP or PEPR1-Km-GFP,
249 indicating that the accumulated PEPR1-Km-GFP signal in the BFA bodies is mainly due to
250 newly protein synthesis and exocytosis (Supplemental Figure 6C). Thus, PEPR1 kinase activity
251 is required for its endocytosis.
252
253 **BAK1 and PEPR1 are co-internalized**
254 To investigate whether BAK1 is internalized together with PEPR1 we used an insertional GFP
255 mutagenesis approach to generate a functional BAK1-GFP fusion by inserting the GFP at
256 different positions into the BAK1 protein (Supplemental Figure 8A and 8B). All constructs
257 were introduced into the *bak1-4* null mutant under the control of the *BAK1* promoter and several
258 independent transgenic lines of each construct were analyzed. Two constructs with GFP
259 insertions into BAK1 between the juxta membrane and the kinase domains (BAK1K253-GFP
260 and BAK1Q273-GFP) and two constructs in which the GFP was inserted into the C-terminal
261 tail of BAK1 (BAK1M580-GFP and BAK1A593-GFP) were selected (Supplemental Figure
262 1A-1C and 9A). All four BAK1 variants rescued the dwarf phenotype of *bak1-4* to some extent.
263 Interestingly, the rosettes of BAK1M580-GFP and BAK1A593-GFP resembled those of
264 Arabidopsis plants with constitutive BR responses (Wang et al., 2001) (Supplemental Figure
265 9A). In the root meristem of all lines, BAK1-GFP localized in the PM, although a more
266 pronounced tonoplast localization was observed in BAK1M580-GFP and BAK1A593-GFP
267 plants (Figure 7A and Supplemental Figure 9B).
268 Of all transgenic lines initially tested in a Pep1-induced root growth inhibition assay, only
269 BAK1K253-GFP and BAK1Q273-GFP partially recovered from the Pep1-triggered root
270 inhibition, although they remained more sensitive to Pep1 than plants expressing the C-
271 terminally tagged BAK1. This phenotype was confirmed with different Pep1 concentrations
272 (Figure 6A and 6B and Supplemental Figure 9C-9E). However, Pep1-triggered MAPK
273 activation in BAK1K253-GFP and BAK1Q273-GFP plants was similar to that of plants
274 expressing BAK1-GFP (Figure 6C). The two mutant lines were more responsive to Pep1

275 application in terms of ROS burst, although they did not produce the ROS levels of the wild-
276 type (Figure 6D). We further examined the responses of these lines to exogenous BRs by
277 assessing the hypocotyl elongation in the dark and the accumulation of dephosphorylated BES1
278 (dBES1), which serves as a readout for BR signaling activation (Yin et al., 2002) (Supplemental
279 Figure 1F and 1G). The hypocotyl growth of BAK1K253-GFP and BAK1Q273-GFP seedlings
280 was sensitive to 100 nM, but not 10 nM brassinolide (BL) and the BES1 dephosphorylation
281 levels were similar to those of the wild-type and BAK-GFP expressing plants, suggesting that
282 the response to exogenous BRs in these lines was not notably affected by the GFP tag.

283 Next, we took advantage of the partially functional BAK1K253-GFP and BAK1Q273-
284 GFP constructs to analyze TAMRA-Pep1 uptake in the corresponding Arabidopsis transgenic
285 plants (Figure 7A and 7B). Interestingly, the endocytosis of TAMRA-Pep1 was restored in
286 BAK1K253-GFP and BAK1Q273-GFP plants compared to BAK1-GFP (Figure 7A and 7B).
287 After a 40-minute chase, TAMRA-Pep1 accumulated in the PM of plants expressing BAK1-
288 GFP, whereas it was clearly internalized in plants expressing BAK1K253-GFP and
289 BAK1Q273-GFP. Based on the recovery of PEPR1 endocytosis in the BAK1K253-GFP and
290 BAK1Q273-GFP lines, we hypothesized that PEPR1 and BAK1 are endocytosed together.
291 Therefore, we analyzed the co-localization between BAK1-GFP and TAMRA-Pep1 (Figure 7C
292 and 7D). Both BAK1K253-GFP and BAK1Q273-GFP co-localized with the TAMRA-Pep1
293 after a 40-minute chase, though not all TAMRA-Pep1 puncta contained the BAK1-GFP (Figure
294 7C). Furthermore, AFCS uptake experiments confirmed that BRI1 endocytosis was not
295 impaired in the BAK1K253-GFP and BAK1Q273-GFP lines (Figure 7E and 7F), consistent
296 with our observations that BR signaling remained unaffected in these plants.

297 To confirm that BAK1 and PEPR1 are internalized together, we purified clathrin-coated
298 vesicles (CCVs) from Arabidopsis *pRPS5A-PEPR1-GFP/pepr1pepr2* seedlings and examined
299 whether BAK1 was present alongside PEPR1 in the enriched CCV fractions after treatment
300 with Pep1 (500 nM for 20 min). Whole Arabidopsis seedlings were used for the isolation of
301 CCVs because Pep1 induced triggered PEPR1-GFP endocytosis in both shoots and roots
302 (Supplemental Figure 10). Analysis of the enriched CCV fractions by immunoblotting revealed
303 that BAK1 was barely detectable in the mock treatment but was enriched in CCVs after Pep1
304 treatment, as was PEPR1 (Figure 7G). Taken together, our data indicate that BAK1 and PEPR1
305 are likely endocytosed together.

306

307 **DISCUSSION**

308

309 Endocytosis controls the amount of functional cell surface receptors and their ligands, acting as
310 a spatial and temporal organizer of signaling (Sigismund et al., 2012). A link between
311 endocytosis and signaling has been established for several Arabidopsis RKs involved in
312 development, such as BRI1 (Irani et al,. 2012), and immunity, including the PRRs, FLS2, EFR,
313 PEPR1 and LYSIN MOTIF-CONTAINING RECEPTOR-LIKE KINASE5 (LYK5) (Erwig et
314 al., 2017; Mbengue et al., 2016; Ortiz-Morea et al., 2016). BAK1 and other SERK family
315 members serve as co-receptors for some of these RKs (Fan et al., 2016). However, despite their
316 crucial role in signaling initiation and transduction (Ma et al., 2016), evidence for their function
317 in endocytosis of the main receptors remains lacking.

318 Transient expression analyses of BAK1 subcellular dynamics in cowpea mesophyll
319 protoplasts (Russinova et al, .2004; Song et al., 2009) revealed that the C-terminal GFP-tagged
320 BAK1 cycles between the PM and the endosomes, where it colocalizes with BRI1 (Russinova
321 et al., 2004). Surprisingly, similar dynamics was not observed in Arabidopsis roots (Bücherl et
322 al., 2013), although, BAK1-GFP localized in the PM, and was able to complement the BR-
323 related defects of the *bak1-4* null mutant (Ntoukakis et al., 2011; Lozano-Durán et al., 2013).
324 Further assessment of BAK1 subcellular dynamics in relation to immunity has been hampered
325 by the observation that the C-terminal GFP-tagged BAK1 is unable to respond to exogenous
326 flg22 and elf18 (Ntoukakis et al., 2011; Lozano-Durán et al., 2013). Here, we show that BAK1-
327 GFP is also impaired in Pep1-triggered responses. Disruption of protein functionality due to a
328 tag fusion has been previously reported in both plant and mammalian systems (Wiśniewska et
329 al., 2006; Hammond et al., 2010; Hurst et al., 2018) and can potentially lead to misinterpretation
330 of the results. Moreover, the functionality of protein fusions may depend on the protein
331 complexes and their respective functions. One possible explanation for the impaired immune
332 responses caused by the C-terminal GFP tag of BAK1 is that it may act in a dominant-negative
333 manner, thereby interfering with receptor complex activation or downstream signal
334 transduction. For example, it could disrupt the recruitment of certain protein partners to the
335 receptor complex, affect PTMs crucial for signaling, or, similar to BAK1-5 protein, stabilize
336 the PEPR1-BAK1 complex at the PM (Schwessinger et al., 2011). Consistent with this, the C-
337 terminal GFP tag was found to impede the phosphorylation on S612 in the C-terminal tail of
338 BAK1, the domain specifically targeted by phosphorylation events required to trigger immune
339 responses in Arabidopsis in response to flg22 and elf18 (Perraki et al., 2018). Additionally,
340 $BAK1^{S612A}$ appeared to co-purify with more FLS2 than the wild-type BAK1 (Perraki et al.,
341 2018). Remarkably, Pep1-induced PEPR1 endocytosis was also severely impaired in the
342 transgenic lines expressing the C-terminal GFP-tagged BAK1, whereas the AFCS BRI1-

343 dependent internalization remained unaffected. Furthermore, BAK1^{AAA} and BAK1^{S612A}
344 mutants deficient in conserved phosphorylation sites, significantly reduced Pep1-induced
345 PEPR1 internalization, providing evidence that BAK1 phosphorylation, necessary for the
346 immune responses (Perraki et al., 2018), is also important for Pep1-triggered PEPR1
347 endocytosis. Supporting this, the semi-dominant *bak1-5* mutant, known to disrupt the immune
348 phosphorylation-dependent function of BAK1 (Perraki et al., 2018), strongly blocked Pep1-
349 triggered PEPR1 endocytosis. Moreover, PEPR1 internalization was only slightly disturbed in
350 the *bak1-4* null mutant, but severely affected in the *bak1-4serk1-1* mutants, suggesting that
351 BAK1 and SERK1 redundantly regulate PEPR1 endocytosis, consistent with earlier studies in
352 tobacco (Mbengue et al., 2016).

353 Examination of the co-localization between the C-terminal GFP-tagged BAK1 and
354 TAMRA-Pep1 revealed that BAK1 localized to the PM, but it did not label the positive
355 compartments of TAMRA-Pep1. This suggest that BAK1 dynamics may be a prerequisite for
356 PEPR1, but not BRI1, endocytosis and signaling, consistent with observations that the C-
357 terminal GFP-tagged BAK1 was functional in terms of BR responses (Ntoukakis et al., 2011;
358 Lozano-Durán et al., 2013). To support this hypothesis and overcome the lack of immune
359 responses caused by the C-terminal GFP tag, we applied an insertional GFP approach to identify
360 a functional fluorescently tagged BAK1 for subcellular dynamics studies. Since the C-terminal
361 tail of BAK1 is important for immune signaling (Wu et al., 2018; Perraki et al., 2018), we
362 inserted the GFP before the critical residues within the C-terminal tail for the generation of
363 BAK1M580-GFP and BAK1A593-GFP, and between the JMD and the KD for that of
364 BAK1K253-GFP and BAK1Q273-GFP.

365 Although BAK1M580-GFP and BAK1A593-GFP rescued the growth defects of the
366 *bak1-4* mutant, they were unable to recover the Pep1-induced root growth inhibition.
367 Interestingly, the rosette phenotype of plants expressing both versions showed extended
368 petioles and curled leaves (Supplemental Figure 9A), resembling plants with high BR signaling
369 (Wang et al., 2001). This result may indicate that the C-terminal tail of BAK1 has a specific
370 role in controlling BR signaling, which warrants further investigation. This contrast with
371 previous reports based on experiments with the BAK1 mutant alleles *suppressor of bir1-1 1*
372 (*sobir)7-1* and *sobir7-3*, which carry mutations in the C-terminal tail of BAK1. These studies
373 revealed that the C-terminal tail of BAK1 is required only for FLS2-mediated defense signaling,
374 but is dispensable for BR responses (Liu et al., 2016).

375 Remarkably, both BAK1K253-GFP and BAK1Q273-GFP versions retained partial
376 responses to exogenous BRs and Pep1, showed dynamics, and restored PEPR1 endocytosis. In

377 addition, BAK1K253-GFP and BAK1Q273-GFP co-localized with TAMRA-Pep1 puncta,
378 suggesting that PEPR1 is endocytosed together with BAK1. Consistent with this co-
379 localization, BAK1 and PEPR1 were detected together in isolated CCVs from Arabidopsis
380 plants after Pep1 treatment. The fact that BAK1 is endocytosed together with PEPR1 raises the
381 possibility that the BAK1-PEPR1 receptor complex maintains signaling from endosomes
382 (Supplemental Figure 11). In mammals, the role of endosomes as signaling platforms is a well-
383 studied, albeit still controversial, phenomenon (Pavlos and Friedman, 2017). However,
384 conclusive evidence for endosomal signaling in plants is still lacking. Further study of the
385 internalization and dynamics of the PEPR1-BAK1 receptor complex may provide additional
386 proof for the existence of similar mechanisms in plants.

387 The ligand-induced endocytosis of PEPR1 depended on its kinase activity, but the
388 phosphorylation relationship between BAK1 and PEPR1 had never been investigated. Protein
389 kinases lacking Arginine in the catalytic loop HxD motif, also known as non-RD kinases, are
390 implicated in immune signaling and may be activated by phosphorylation-dependent
391 conformational changes in the receptor cytoplasmic domain, but not by an activation loop
392 phosphorylation (Bender et al., 2021). For example, BAK1 phosphorylates the non-RD kinase
393 EFR in the activation loop to stabilize its active conformation, allowing EFR in turn to
394 allosterically activate BAK1 but not vice versa (Wang et al., 2014; Schwessinger et al., 2011;
395 Mühlenbeck et al., 2024). Unlike other PRRs, PEPR1 is an RD kinase with strong kinase
396 activity *in vitro* and has been shown to phosphorylate various partners, such as BIK1 (Liu et
397 al., 2013) and the REGULATOR OF G SIGNALLING PROTEIN1 (RGS1) (Tunc-Ozdemir et
398 al., 2017). We found that PEPR1 can phosphorylate BAK1 *in vitro*, but, surprisingly, not vice
399 versa. This is remarkable, because BAK1 trans-phosphorylates most of its co-receptors,
400 including the non-RD kinases FLS2 (Lin et al., 2014), EFR (Wang et al., 2014; Schwessinger
401 et al., 2011), the RD kinase BRI1 (Wang et al., 2008), and other substrates, such as NUCLEAR
402 SHUTTLE PROTEIN-INTERACTING KINASE1 (NIK1) (Li et al., 2019), BIK1 (Liu et al.,
403 2017), and H^+-ATPASE ISOFORM2 (AHA2) (Pei et al., 2022). Although BAK1 did not
404 phosphorylate PEPR1, the presence of the BAK1 kinase visibly increased PEPR1
405 phosphorylation *in vitro*, comparable to the observed *in vivo* increase in phosphorylation at
406 T896 in PEPR1 when co-expressed with BAK1 in the presence of Pep1. Additionally, PEPR1
407 kinase reduced BAK1 phosphorylation *in vitro*. Likewise, FLS2 and EFR reduced BAK1 kinase
408 activity *in vitro* (Wang et al., 2014). Interestingly, the mutual influence observed between
409 PEPR1 and BAK1 was disrupted in the BAK1 phosphorylation mutants. For example, PEPR1
410 phosphorylation increased in the presence of $BAK1^{S612A}$ and the PEPR1 kinase slightly

411 decreased the phosphorylation of BAK1^{S612A}. Whereas BAK1-5 and BAK1^{AAA} kinases had
412 comparable activity, they did not affect PEPR1 phosphorylation. However, PEPR1 kinase
413 reduced the phosphorylation of BAK1-5, whereas its effect on BAK1^{AAA} was less clear. Taken
414 together, the mutual trans-phosphorylation mechanism for activation of RKs complexes, as in
415 BRI1-BAK1 and FLS2-BAK1, might not apply to PEPR1-BAK1 and requires further
416 investigation.

417 In conclusion, our study demonstrates that the PEPR1 endocytosis is controlled by the
418 co-receptor BAK1 via phosphorylation in its C-terminal tail, which is indispensable for Pep1-
419 mediated signaling. This raises the question of the possible mechanism underlying this
420 regulation (Supplemental Figure 11). It is tempting to speculate that BAK1 counteracts an as-
421 yet-unknown component of the receptor complex that negatively regulates PEPR1 endocytosis.
422 In line with this hypothesis, BAK1 restricts the activation of the LRR RK, BAK-TO-LIFE 2
423 (BTL2) through specific phosphorylation to maintain cellular integrity (Yu et al., 2023).
424 However, whether BTL2 affects endocytosis of the main receptor remains unclear. BAK1 can
425 also regulate specific PTMs in PEPR1 that positively regulate ligand-induced receptor
426 endocytosis, such as phosphorylation or ubiquitination (Dubeaux and Vert, 2017). Notably, in
427 contrast to other BAK1 receptor partners, PEPR1 can phosphorylate BAK1 to reduce its
428 activity. Additionally, the immune-required phosphorylation of BAK1 is not necessary for
429 BRI1 endocytosis, suggesting that BAK1 employs different mechanisms to regulate different
430 receptor partners or may even be dispensable for BRI1 internalization. Nevertheless, the precise
431 mechanism by which BAK1 controls PEPR1 endocytosis remains to be elucidated. Whether
432 BAK1 has a similar effect on other PRRs is unclear. Some conflicting evidence exists that
433 BAK1 is essential for ligand-induced endocytosis of certain PRRs in transient assays (Mbengue
434 et al., 2016), but it is not required for FLS2 recycling in Arabidopsis leaves, regardless of the
435 ligand presence (Beck et al., 2012). Furthermore, using the newly designed and partially
436 functional BAK1-GFP lines, it would be interesting to investigate BAK1 dynamics within
437 different immune receptor complexes, such as FLS2 and EFR. Our findings suggest that the
438 ligand-induced endocytosis of the main receptor is regulated in a co-receptor-dependent
439 manner.
440

441 **METHODS**

442

443 **Plant material, growth conditions and reagents**

444 All mutants and transgenic lines used in this study were in the background of the *Arabidopsis*
445 *thaliana* (L.) Heynh. (accession Columbia-0 [Col-0]). Seeds were surface-sterilized with
446 chlorine gas and then placed on plates with half-strength Murashige and Skoog (½MS) medium
447 containing 0.8% (w/v) agar, and 2.5 mM methyl ester sulfonate at pH 5.7. After vernalization
448 for 2 days at 4°C, the plates were moved to the growth chamber at 22°C in a 16 h/8 h light/dark
449 cycle with a light intensity of 120 µE m^{-2} s^{-1}. The following mutant and transgenic Arabidopsis
450 lines have been described previously: *pRPS5A-PEPR1-GFP/pepr1pepr2* (Ortiz-Morea *et al*,
451 2016); *bak1-4* (Chinchilla *et al*, 2007); *bak1-5* (Schwessinger *et al*, 2011); *serk1-1bak1-4*
452 (Meng *et al*, 2015); *bak1-3/serk4-1* (Du *et al,* 2016); *serk1-1(+/-)serk2-1bak1-4* (Meng *et al*,
453 2015); *serk1-1serk2-1(+/-)serk4-1* (Meng *et al*, 2015); *pBAK1-BAK1/bak1-4* (Perraki *et al*,
454 2018); *pBAK1-BAK1*^{S612A}*/bak1-4* (Perraki *et al*, 2018); and *pBAK1-BAK1*$^{S602A;T603A;S604A}$*/bak1-*
455 *4* (Perraki *et al*, 2018). The *pRPS5A-PEPR1-GFP/pBAK1-BAK1*^{S612A}*/bak1-4* and *pRPS5A-*
456 *PEPR1-GFP/pBAK1-BAK1*$^{S602A;T603A;S604A}$*/bak1-4* lines were generated by crossing *pRPS5A-*
457 *PEPR1-GFP/bak1-4* with either *pBAK1-BAK1*^{S612A}*/bak1-4* or *pBAK1-BAK1*$^{S602A;T603A}$
458 $^{;S604A}$*/bak1-4*. For phenotypic analysis, plants were grown in soil in a growth chamber at 22°C,
459 58% relative humidity, and a 16 h light/8 h light/dark photoperiod for 6 weeks. N-(3-
460 triethylammoniumpropyl)-4-(6-(4-(diethylamino) phenyl) hexatrienyl) pyridinium dibromide
461 (FM4-64; 2 mM stock in purified water; Invitrogen), BFA [50 mM stock in dimethyl sulfoxide
462 (DMSO); Sigma-Aldrich], CHX (50 mM stock in DMSO; Sigma-Aldrich), BL (10 mM stock
463 in DMSO; Wako Pure Chemical Industries and OlChemlm) were used at the concentrations
464 indicated in the figure legends.
465

466 **Plasmid construction**

467 cDNA or genomic DNA from Arabidopsis Col-0 was used as template for PCR cloning. The
468 *BAK1* promoter was amplified and introduced into the *pDONRP4-P1R* donor vector to build
469 *pDONRP4-P1R-pBAK1*. The *BAK1* coding sequence without stop codon was cloned into
470 *pDONR221* to generate *pDONR221-BAK1* that was used as a template together with
471 *pDONRP2-P3R-GFP* to generate the BAK1 insertional GFP versions by overlapping PCR and
472 subcloned into *pDONR221* to generate *pDONRP1P2-BAK1K253-GFP, pDONRP1P2-*
473 *BAK1Q273-GFP, pDONRP1P2-BAK1M580-GFP* and *pDONRP1P2-BAK1A593-GFP.* The
474 destination vectors were generated by recombining the *pH7m24GW,3, pDONRP4-P1R-pBAK1,*
475 and *pDONRP1P2-BAK1-GFP* versions.

476 For protein purification, the CD-encoding sequences of BAK1were amplified and
477 introduced into *pDONR221* to generate *pDONR221-BAK1-CD* that was used as template to

478 generate *BAK1-5(C408Y)-CD* and *BAK1-Km(D416N)-CD* by overlapping PCR and subcloned
479 into *pDONR221*. The entry clones *pDONR221-BAK1-CD, pDONR221-BAK1-5-CD,*
480 *pDONR221-BAK1-Km-CD, pDONR221-BAK1*^{S612A}*-CD* (Perraki *et al*, 2018), and *pDONR221-*
481 *BAK1* $^{S602A;T603A;S604A}$*-CD* (Perraki *et al*, 2018) were recombined into the bacterial expression
482 vector *pOPINM* (Berrow *et al*, 2007) containing the His6-MBP tag. Sequences encoding CDs
483 of *PEPR1* and *PEPR1-Km(K855E)* were amplified with specific primers containing restriction
484 sites. The point mutations were generated by means of overlapping PCR. The PCR products
485 and the plasmid *pGEX-5x1* were digested with the restriction enzymes EcoRI and BamHI
486 (FastDigest; Thermo Fisher Scientific). The linearized and purified plasmid was
487 dephosphorylated by Thermosensitive Alkaline Phosphatase (Promega). PCR products and
488 plasmid were ligated by T4 DNA ligase (Invitrogen) to generate *pGEX-5x1-PEPR1-CD* and
489 *pGEX-5x1-PEPR1-Km-CD*. Constructs were introduced into the *Escherichia coli* strain
490 Rosetta2 for protein production. All primers used are listed in Table EV1. All clones were
491 confirmed by sequencing.
492
493 **Generation of transgenic plants**
494 Plants were transformed with the *Agrobacterium tumefaciens* strain C58C1 by means of the
495 floral dip method (Clough & Bent, 1998). BAK1 constructs were transformed into the *bak1-4*
496 null mutant Transformed plants were selected on ½MS agar medium containing 50 mg/l
497 hygromycin.
498
499 **Peptides**
500 The peptide Pep1 (ATKVKAKQRGKEKVSSGRPGQHN) with a HPLC purity of 95% and the
501 peptide Pep1 labelled with 5'- carboxytetramethylrhodamine at the N-terminal (TAMRA-Pep1)
502 with a HPLC purity of 95% were purchased from EZBiolab. The peptides were dissolved in
503 water to obtain peptide stocks of 1 mM and further diluted with ½MS medium.
504
505 **Root and hypocotyl growth assays**
506 Seeds were sown on ½MS solid medium, stratified for 2 days at 4°C in the dark, and placed
507 vertically in the light. Four days after germination, seedlings were transferred to solid ½MS
508 medium supplemented with or without the indicated amount of Pep1 and incubated for a further
509 3 days, whereafter the plates were scanned. For the hypocotyl, seeds were sown directly on ½
510 MS medium supplemented with either increasing concentrations of BL or (DMSO), stratified
511 for 2 days at 4ºC in the dark. The plates were moved to growth chamber at 22ºC and placed

512 vertically in light for 6 h. Then, the plates were wrapped in aluminum foil for dark condition
513 and kept vertically in growth chamber at 22°C for 5 days. For root and hypocotyl
514 measurements, plates were scanned and the scanned images were processed and evaluated with
515 the ImageJ software and plotted relative to the untreated control.
516
517 **Detection of reactive oxygen species (ROS) burst**
518 For ROS burst assay (Zhang *et al*, 2010), leaf discs (5 mm in diameter) were collected from the
519 third or fourth true leaves of four-week-old Arabidopsis plants grown in soil. These discs were
520 placed into individual wells of a 96-well plate, each containing 100 µL of distilled water, and
521 left to incubate overnight under a 12-hour light/12-hour dark cycle. The next day, the water was
522 replaced with 100 µL of a reaction solution composed of 50 µM luminol and 10 µg/mL
523 horseradish peroxidase (Sigma-Aldrich, USA), with or without the addition of Pep1 at
524 concentrations as indicated. Luminescence signals were detected using a GloMax-Multi System
525 luminometer (Promega, USA).
526
527 **MAP kinase assay**
528 Arabidopsis seedlings were germinated on ½ MS medium and, after three or five days, were
529 transferred to a 12-well plate with ½ MS medium. Following 1 hour of conditioning, the
530 medium was supplemented with 100 nM Pep1. Seedlings were incubated with peptides for the
531 indicated time points, whereafter they were harvested and frozen in liquid N_2. Frozen plant
532 material was ground and the extraction buffer [50 mM Tris, pH 7.5, 200 mM NaCl, 1 mM
533 EDTA, 10% (v/v) glycerol, 0.1% (v/v) Tween 20, 1 mM phenylmethylsulfonyl fluoride, 1 mM
534 DTT, 1×PhosSTOP™ (4906837001; Sigma-Aldrich) and 1×cOmplete™ ULTRA Tablets
535 (5892791001; Sigma-Aldrich)] was added at the ratio of 2 µL per mg tissue (1:2 w:v). Samples
536 were vortexed and centrifuged at 13000*g* for 30 min. Protein concentration was quantified in
537 the supernatant with the Qubit protein assay kit (Thermo Fischer Scientific). Equal amounts of
538 proteins (30 µg) were separated on 7.5% sodium dodecyl sulphate (SDS)/polyacrylamide gel
539 electrophoresis (PAGE) and transferred onto a nitrocellulose membrane (Bio-Rad). After
540 blocking with 3% bovine serum albumin, membranes were incubated overnight with primary
541 antibodies against anti-phospho- p44/42 (1:2500; Cell Signaling Technology). Horseradish
542 peroxide (HRP)-conjugated anti-rabbit secondary antibody (1:10000; GE Healthcare;) was used
543 and signals were detected with the SuperSignal™ West Femto Maximum Sensitivity Substrate
544 (34095; Thermo Fisher Scientific). Antibodies were stripped in 1:1 (v:v) 10% SDS and 100 mM
545 glycine-HCl (pH 2.5) solution, washed five times, and reblotted with anti-MPK6 antibody

546 (1:8000; Sigma-Aldrich) and anti-MPK3 antibody (1:2500; Sigma-Aldrich). HRP-conjugated
547 anti-rabbit secondary antibody (1:10000; GE Healthcare) was used and signals detected with
548 Western Lightning Plus Electrochemiluminescence (NEL105001EA; PerkinElmer). All blots
549 were imaged in a ChemiDoc XRS+ imaging system (Bio-Rad).
550
551 **Immunoblots**
552 The Arabidopsis seedlings were ground in liquid N_2, resuspended in total protein extraction
553 buffer (25 mM Tris-HCl, pH 7.5, 150 mM NaCl, and Roche cOmplete ULTRA protease
554 inhibitor cocktail, Roche PhosSTO tablet) in a 1:2 (w/v) ratio, and centrifuged at 15,000*g*. The
555 supernatants were mixed with required amount of 4× NuPAGE lithium dodecyl sulphate (LDS)
556 sample buffer (Invitrogen) and 10× NuPAGE sample-reducing agent (Invitrogen), heated at
557 70°C for 10 min, and loaded onto 4-20% Mini-PROTEAN TGX precast gels. The proteins were
558 transferred to nitrocellulose membranes by means of the Trans-Blot® Turbo™ Transfer System
559 (Bio-Rad). For protein detection, the following antibodies were used: monoclonal α-GFP-HRP
560 (1/5,000; Miltenyi Biotech), monoclonal α-tubulin (1/10,000; Sigma-Aldrich), α-BES1
561 (1:4,000; Yin et al., 2002), α-BAK1 (1/5,000; custom-made by Eurogentec). Blots were
562 developed with Western Lightning Plus-ECL, Enhanced Chemiluminescence Substrate
563 (Perkin-Elmer), and imaged with the Bio-Rad ChemiDoc XRS+molecular imager.
564
565 **TAMRA-Pep1 internalization assay and image analysis**
566 Five-day-old seedlings were dipped into 500 µl of 100 nM TAMRA-Pep1 dissolved in ½MS
567 medium for 10 sec, washed with ½MS liquid medium three times, and kept in 500 µl of ½MS
568 medium over a Parafilm piece in a Petri plate. The epidermal cells of the root meristematic zone
569 were imaged at the indicated time points with a laser scanning confocal microscope SP8X
570 (Leica) equipped with an HC PL APO CS2 40×/1.10 water-corrected objective with 4× digital
571 zoom. The excitation wavelength was 559 nm by white light laser. Emission was detected at
572 570-670 nm by hybrid detectors (Leica). For the image quantification with FIJI
573 (https://imagej.net/software/fiji/), the first images were converted to 8-bit images;
574 subsequently, the entire plasma membranes of individual cells were selected with the brush tool
575 size 10 pixels and the intracellular spaces with the polygon selection tool. The number of the
576 5% highest pixels was obtained for both PM and intracellular space. These values were used to
577 obtain a ratio. Ten epidermal cells from five plants were quantified.
578
579 **AFCS uptake assays and image analysis**

580 The AFCS uptake assay was done as previously described (Irani *et al*, 2014) with modifications.
581 Six-day-old seedlings grown on solid ½MS were transferred to 200 µl of liquid ½MS on a
582 Parafilm piece placed in a Petri plate, humidified with wet laboratory wipes for 10 min. The
583 medium was replaced with ½MS supplemented with 30 µM AFCS for 40 min (pulse).
584 Seedlings were washed six times and chased for 30 min on ½MS followed by imaging.
585 Epidermal cells of the root meristematic zone were imaged with the laser scanning confocal
586 microscope SP8X (Leica) equipped with an HC PL APO CS2 63×/1.20 water-corrected
587 objective with 4× digital zoom. The excitation wavelength was 633 nm by white light laser.
588 Emission was detected at 650-700 nm by hybrid detectors (Leica). For fluorescence signal
589 measurements in vacuoles, stacks of four to six slices of 1.5 µm were obtained. Images were
590 analyzed and signals quantified with the Fiji/ImageJ software. Four to six slices covering the
591 epidermal cell layer were merged by means of maximum projection. The images were
592 processed with Gaussian blur filter (1) and Subtraction Background (100). Rectangular regions
593 of interest were determined omitting over-stained regions, such as the lateral root cap. The
594 signal intensity was quantified in seven to nine seedlings per genotype.
595
596 **Protein production and purification**
597 For GST-tagged protein production, the *E. coli* strain Rosetta2 harboring each of the plasmids
598 pGEX-5×1-PEPR1-CD, pGEX-5×1-PEPR1-Km-CD or *pDEST15-BIK1-Km(KK105AA*) was
599 grown in Luria-Bertani (LB) medium supplemented with carbenicillin (100 µg/ml) at 37˚C until
600 an optical density OD_{600} of 0.6-0.8. Protein production was induced with 1 mM isopropyl β-D-
601 1-thiogalactopyranoside (IPTG) at 16°C overnight, and shaking at 200 rpm. The bacterial
602 culture was pelleted (15 min, 5000*g*) and frozen at -20°C. The cells were resuspended in
603 extraction buffer [50 mM Tris-HCl, pH 8.5, 100 mM NaCl, 1 mM EDTA, 1 mM DTT, protease
604 inhibitor cocktail tablet (cOmplete ULTRA Tablets; Roche), 1 mg/ml lysozyme, 0.4 mM
605 PMSF, 1% Triton X-100] and incubated on ice for 60 min. Resuspended cells were sonicated
606 until the solution became fluid and clear. The lysate was centrifuged (30 min, 12000*g* at 4˚C)
607 and the supernatant was transferred to a new tube. Proteins were purified with Glutathione
608 Sepharose® 4B (GE Healthcare). Glutathione Sepharose slurry (300 µl) was washed twice with
609 binding buffer (50 mM Tris-HCl, pH 8.5, 100 mM NaCl, 1 mM EDTA, and 1 mM DTT) by
610 addition of 5 ml buffer for 1 ml slurry. After washing, the slurry was added to the lysate and
611 incubated for 60 min on an end-to-end rotor at 4˚C. After incubation, slurry was spun down
612 (5 min, 500*g*) and washed twice with 10 ml washing buffer A (50 mM Tris-HCl, pH 8.5,
613 100 mM NaCl, 1 mM EDTA, 1 mM DTT, and 0.1% [v/v] Triton X-100) for 15 min on an end-

614 to-end rotor at 4°C. The slurry was further washed twice with 10 ml binding buffer (50 mM
615 Tris-HCl, pH 8.5, 100 mM NaCl, 1 mM EDTA, 1 mM DTT) for 15 min on an end-to-end rotor
616 at 4˚C. For elution, the slurry was incubated for 10 min at room temperature on an end-to-end
617 rotor with 500 µl elution buffer (50 mM Tris-HCl, pH 8.5, 100 mM NaCl, 1 mM EDTA, 1 mM
618 DTT, 20 mM freshly prepared gluthatione, pH 8.0). The elution was repeated three times and
619 the three eluates were pooled and concentrated with Amicon® Ultra 30K (Millipore) until
620 500 µl was obtained.

621 For His6-MBP-tagged proteins, *E. coli* strain Rosetta2 harboring the plasmid *pOPNIM-*
622 *BAK1-CD, pOPNIM-BAK1-5-CD, pOPNIM-BAK1-Km-CD, pOPNIM-BAK1*^{S612A}*-CD,* and
623 *pOPNIM-BAK1* $^{S602A;T603A;S604A}$*-CD* was grown in LB medium supplemented with 100 µg/ml
624 carbenicillin at 37˚C until OD_{600} = 0.6-0.8. Protein production was induced with 1 mM of IPTG
625 at 16˚C overnight, with shaking at 200 rpm. The bacterial culture was pelleted (15 min, 5000*g*)
626 and frozen at -20˚C. The cells were resuspended in extraction buffer [20 mM Tris-HCl, pH 8.5,
627 200 mM NaCl, 1 mM EDTA, 1 mM DTT, protease inhibitor cocktail tablet (cOmplete ULTRA
628 Tablets; Roche), 1 mg/ml lysozyme, 0.4 mM PMSF] and incubated on ice for 60 min.
629 Resuspended cells were sonicated until the solution became fluid and clear. The lysate was
630 centrifuged (30 min, 12000*g* at 4˚C) and the supernatant was transferred to a new tube. Proteins
631 were purified with mylose resin (NEB). Amylose slurry was washed three times with wash
632 buffer (20 mM Tris-HCl pH 8.5, 200 mM NaCl, 1 mM EDTA, and 1 mM DTT) and then
633 incubated with the lysate for 60 min on an end-to-end rotor at 4˚C. After incubation, the slurry
634 was spun down (5 min, 500*g*) and washed three times with 10 ml of wash buffer for 15 min on
635 an end-to-end rotor at 4˚C. For elution, the amylose slurry was incubated for 10 min at room
636 temperature on an end-to-end rotor with 1 ml elution buffer (20 mM Tris-HCl pH 8.5, 200 mM
637 NaCl, 1 mM EDTA, 1 mM DTT, and 10 mM maltose). Elution was repeated three times and
638 the three eluates were pooled and concentrated with Amicon® Ultra 30K (Millipore) until
639 500 µl was obtained.
640

641 ***In vitro* kinase assay and in-gel trypsin digestion for mass spectrometry (MS)**

642 The *in vitro* kinase assay was carried out by mixing either GST-PEPR1-CD or GST-PEPR1-
643 Km-CD with His6-MBP-BAK1-CD, His6-MBP-BAK1-5-CD, His6-MBP-BAK1^{S612A}-CD,
644 and His6-MBP-BAK1^{AAA}-CD; all the combinations, including the proteins alone, were tested
645 for autophosphorylation. CDs were mixed with 5 µl of [γ-^{32}P] ATP (1 µCi/µl) and the kinase
646 assay buffer (50 mM Tris-HCl, pH 7.5, 100 mM NaCl, 10 mM $MgCl_2$, and 10 µM ATP) was
647 added in 30 µl final volume. The reaction was incubated for 1 h at 25°C and stopped by addition

648 of 10 µl loading buffer 4× [NuPAGE® LDS Sample Buffer (4×)] and 5 µl of 10× reduction
649 buffer [NuPAGE® Sample Reducing Agent (10×)]. Samples were loaded on 4-20% precast
650 SDS-PAGE gels (Bio-Rad). The gels were stained with Bio-Safe Coomassie Brilliant Blue
651 (CBB) (Bio-Rad), dried between cellophane plastic sheets, and [γ-^{32}P] was detected by
652 autoradiography. To examine the phosphorylation sites by MS, an *in vitro* kinase experiment
653 with non-radioactive ATP was conducted after the previously described steps. After the kinase
654 reaction had ended, the samples were segregated by SDS-PAGE and then stained with CBB.
655 Thereafter, in-gel trypsin digestion was carried out, as outlined previously. The resulting
656 digested peptides were purified with OMIX C18 Pipette Tips (Agilent Technologies) and
657 subsequently subjected to a liquid chromatography-tandem MS (MS/MS).
658
659 **Detection of protein phosphorylation in the *Nicotiana benthamiana* leaf epidermis**
660 Agrobacteria containing *P19*, *p35S-PEPR1-Km-GFP* or *p35S-BAK1-mCherry* were co-
661 infiltrated into *Nicotiana benthamiana* leaves with the combination shown in the figure. After
662 60 hours, leaves were treated with water or 500 nM Pep1 for 15 min by injection before
663 harvesting. Four biologically replicated samples per experimental group were ground with
664 liquid nitrogen. Total protein was extracted from 5 mL of compacted plant powder using
665 extraction buffer [50 mM Tris-HCl pH7.5, 150 mM NaCl, 1 mM EDTA, 1% NP-40, 5%
666 glycerol, protease inhibitor cocktail (Roche) and PhosSTOP (Roche)]. Immunoprecipitation
667 was performed with GFP-Trap magnetic agarose (ChromoTek) followed by 3 washes with wash
668 buffer (50 mM Tris-HCl pH7.5, 150 mM NaCl, 1 mM EDTA and 1% NP-40) and 1 wash with
669 50 mM TEAB pH8.0 (Thermo Fischer). Protein was eluted on beads using 0.5 µg trypsin, and
670 then alkylated of cysteine residues using 15 mM tris(carboxyethyl)phosphine (TCEP, Pierce)
671 and 30 mM iodoacetamide (Sigma-Aldrich). The peptides were completely digested by
672 incubation with 0.5 µg trypsin for 16 hours and desalting with OMIX C18 pipette tips (Agilent
673 Technologies). The LC-MS/MS analyses were carried out as described previously (Vu *et al.*
674 2021). Peptide searches were performed using MaxQuant (version 2.1.4.0) on a high
675 performance computer (HPC-UGent) against a database containing all *Nicotiana benthamiana*
676 protein sequences from UniProt (Proteome ID: UP000084051) and the *Arabidopsis thaliana*
677 protein sequences of PEPR1-Km-GFP and BAK1-mCherry.
678
679 **Database searching and data analysis**
680 MS/MS spectra were searched with the BL21(DE3) proteome database and the sequences of
681 GST-PEPR1-CD, GST-PEPR1-CD-kinase dead, HIS6-MBP-BAK1-CD, and HIS6-MBP-

682 BAK1-Km-CD with the MaxQuant software (version 1.6.17.0) by means of the UseGalaxy.be
683 server. MaxQuant settings can be found in Dataset EV1. The 'Phospho (STY).txt' output file
684 generated by the MaxQuant search was loaded into the Perseus software (version 1.6.7.0) for
685 analysis. All the data were selected first by a localization probe cut-off of >0.75. The Log2-
686 transformed phosphosite intensities were used for further analysis. The 'proteinGroups.txt' file
687 was also loaded into the Perseus software (version 1.6.7.0) for analysis. The label-free
688 quantification (LFQ) intensities were loaded and transformed by Log2 for further analysis.
689

690 **CCV Purification**

691 Seven-day-old *pRPS5A-PEPR1-GFP/pepr1pepr2* seedlings were grown in ½MS. A sample of
692 30 g was ground at 4°C and fractionated to purify CCVs as described previously (Mosesso *et*
693 *al*, 2019). Samples collected during the purification and the final CCV fraction were analyzed
694 by immunoblot analysis with antibodies against organelles and/or cellular compartments. The
695 antibodies used were: HRP-coupled monoclonal α-GFP (1:2,500; Miltenyi Biotech), α-CHC
696 (1:5,000; Santa Cruz Biotechnologies), α-H^+ ATPase (1:5,000; Agrisera), α-V-ATPase
697 (1:5,000; Agrisera), and α-BiP (1:2,000; Agrisera).
698

699 **RT-qPCR**

700 Total RNA was extracted from approximately 100 mg of 5-day-old seedlings with the RNeasy
701 kit (Qiagen). cDNA was synthesized from 1000 ng of RNA with the qScript cDNA Supermix
702 (Quantabio). The resulting cDNA was diluted to 1:5 with nuclease-free water. RT-qPCRs were
703 run with SYBR green I Master kit (Roche) on a LightCycler 480 (Roche). Expression was
704 normalized to that of *ACTIN2* and *GAPDH* genes. The cycling conditions were as follows:
705 preincubation at 95°C for 10 min; 45 amplification cycles at 95°C for 10 s, 60°C for 15 s, and
706 72°C for 15 s; melting curve at 95°C for 1 s, and 65°C for 1 s, followed by cooling at 40°C for
707 10 s. The integrity of the PCR amplicon was confirmed by melting curve analyses. The primers
708 used are listed in Table EV1
709

710 **Quantification and statistical analysis**

711 All statistical analyses were carried out in GraphPad Prism 9. Statistically significant
712 differences were determined by one-way or two-way Analysis of Variance (ANOVA) test.
713

714 **Data availability**

No data were deposited in external repositories. Data used for quantifications as well as full Western blots can be found in the source data file. All material will be made available upon request to the corresponding author (eugenia.russinova@psb.vib-ugent.be).

SUPPLEMENTAL INFORMATION

Supplemental information is available online

FUNDING

This work was supported by special research funding from the Flemish Government and funding from the Student Program-Graduate Studies Plan Program from the Coordination for the Improvement of Higher Education Personnel (Brazil) for a for a joint doctorate fellowship at Ghent University and University of São Paulo to FAO-M; the European Union's Horizon 2020 research and innovation program under the Marie Sklodowska-Curie grant agreement (No 101023079 'ENDOLOGISTIC') to SY; PEW Latin American Fellows Program to FAO-M, the National Science Foundation (NSF) (MCB-1906060) to PH, and NSF (IOS-2049642) to LS, the China Scholarship Council for a predoctoral fellowship (201706350153) and a UGent BOF doctoral mandate (01CD7122) to XX, and the Research Foundation-Flanders (G003720N) to ER. The computational resources (Stevin Supercomputer Infrastructure) and services used in this work were provided by the VSC (Flemish Supercomputer Center), funded by Ghent University, FWO and the Flemish Government – department EWI.

AUTHOR CONTRIBUTIONS

L.A.N.C., F.A.O.-.M. and E.R. initiated and designed the experiments. L.A.N.C. did most of the work. X. X., S.-L. Y. and I.D.S. identified the *in vitro* / *in vivo* phosphorylation sites. S. Y. did phenotypic analysis. I.Y. performed some MAPK and ROS assays. I. D.S., P.H., L.S., and E.R. provided supervision, funding and analyzed the data. L.A.N.C. and E.R. wrote the manuscript and all authors revised it.

ACKNOWLEDGEMENTS

We thank Yanhai Yin for providing the α-BES1 antibody, Cyril Zipfel for published materials, Guilherme Perreira de Oliveira for technical help, Daniel Scherer de Moura and Daniel V. Savatin for constructive discussions, and Martine De Cock for help in preparing the manuscript.

DISCLOSURE AND COMPETING INTERESTS STATEMENT

749 The authors declare that they have no conflict of interest.

750

751 **REFERENCES**

752 Bartels S, Boller T (2015) Quo vadis, Pep? Plant elicitor peptides at the crossroads of
753 immunity, stress, and development. *J Exp Bot* 66: 5183-5193
754 Bartels S, Lori M, Mbengue M, van Verk M, Klauser D, Hander T, Böni R, Robatzek S,
755 Boller T (2013) The family of Peps and their precursors in *Arabidopsis*: differential
756 expression and localization but similar induction of pattern-triggered immune responses.
757 *J Exp Bot* 64: 5309-5321
758 Beck M, Zhou J, Faulkner C, MacLean D, Robatzek S (2012) Spatio-temporal cellular
759 dynamics of the *Arabidopsis* flagellin receptor reveal activation status-dependent
760 endosomal sorting *Plant Cell* 24: 4205-4219
761 Bender KW, Couto D, Kadota Y, Macho AP, Sklenar J, Derbyshire P, Bjornson M, DeFalco
762 TA, Petriello A, Font Farre M *et al* (2021) Activation loop phosphorylation of a non-RD
763 receptor kinase initiates plant innate immune signaling. *Proc Natl Acad Sci USA* 118:
764 e2108242118
765 Berrow NS, Alderton D, Sainsbury S, Nettleship J, Assenberg R, Rahman N, Stuart DI,
766 Owens RJ (2007) A versatile ligation-independent cloning method suitable for high-
767 throughput expression screening applications. *Nucleic Acids Res* 35: e45
768 Bücherl CA, van Esse GW, Kruis A, Luchtenberg J, Westphal AH, Aker J, van Hoek A,
769 Albrecht C, Borst JW, de Vries SC (2013) Visualization of BRI1 and BAK1(SERK3)
770 membrane receptor heterooligomers during brassinosteroid signaling *Plant Physiol* 162:
771 1911-1925
772 Chinchilla D, Zipfel C, Robatzek S, Kemmerling B, Nürnberger T, Jones JDG, Felix G,
773 Boller T (2007) A flagellin-induced complex of the receptor FLS2 and BAK1 initiates
774 plant defence. *Nature* 448: 497-500
775 Choi J, Tanaka K, Cao Y, Qi Y, Qiu J, Liang Y, Lee SY, Stacey G (2014) Identification of a
776 plant receptor for extracellular ATP. *Science* 343: 290-294
777 Claus LAN, Savatin DV, Russinova E (2018) The crossroads of receptor-mediated signaling
778 and endocytosis in plants. *J Integr Plant Biol* 60: 827-840
779 Clough SJ, Bent AF (1998) Floral dip: a simplified method for *Agrobacterium*-mediated
780 transformation of *Arabidopsis thaliana*. *Plant J* 16: 735-743

781 Du J, Gao Y, Zhan Y, Zhang S, Wu Y, Xiao Y, Zou B, He K, Gou X, Li G *et al.* (2016)
782 Nucleocytoplasmic trafficking is essential for BAK1- and BKK1-mediated cell-death
783 control. *Plant J* 85: 520-531
784 Dubeaux G, Neveu J, Zelazny E, Vert G (2018) Metal sensing by the IRT1 transporter-
785 receptor orchestrates its own degradation and plant metal nutrition. *Mol Cell* 69: 953-964
786 Dubeaux G, Vert G (2017) Zooming into plant ubiquitin-mediated endocytosis. *Curr Opin*
787 *Plant Biol* 40: 56-62
788 Ekanayake G, Smith JM, Jones KB, Stiers HM, Robinson SJ, LaMontagne ED, Kostos PH,
789 Cornish PV, Bednarek SY, Heese A (2021) DYNAMIN-RELATED PROTEIN DRP1A
790 functions with DRP2B in plant growth, flg22-immune responses, and endocytosis. *Plant*
791 *Physiol* 185: 1986-2002
792 Erwig J, Ghareeb H, Kopischke M, Hacke R, Matei A, Petutschnig E, Lipka V (2017) Chitin-
793 induced and CHITIN ELICITOR RECEPTOR KINASE1 (CERK1) phosphorylation-
794 dependent endocytosis of *Arabidopsis thaliana* LYSIN MOTIF-CONTAINING
795 RECEPTOR-LIKE KINASE5 (LYK5). *New Phytol* 215: 382-396
796 Fan M, Wang M, Bai M-Y (2016) Diverse roles of SERK family genes in plant growth,
797 development and defense response. *Sci China Life Sci* 59: 889-896
798 Geldner N, Anders N, Wolters H, Keicher J, Kornberger W, Muller P, Delbarre A, Ueda T,
799 Nakano A, Jürgens G (2003) The *Arabidopsis* GNOM ARF-GEF mediates endosomal
800 recycling, auxin transport, and auxin-dependent plant growth. *Cell* 112: 219-230
801 Hammond JW, Blasius TL, Soppina V, Cai D, Verhey KJ (2010) Autoinhibition of the
802 kinesin-2 motor KIF17 via dual intramolecular mechanisms. *J Cell Biol* 189: 1013-1025
803 Hou S, Liu Z, Shen H, Wu D (2019) Damage-associated molecular pattern-triggered
804 immunity in plants. *Front Plant Sci* 10: 646
805 Huffaker A, Dafoe NJ, Schmelz EA (2011) ZmPep1, an ortholog of Arabidopsis elicitor
806 peptide 1, regulates maize innate immunity and enhances disease resistance. *Plant*
807 *Physiol* 155: 1325-1338
808 Huffaker A, Pearce G, Veyrat N, Erb M, Turlings TCJ, Sartor R, Shen Z, Briggs SP, Vaughan
809 MM, Alborn HT *et al* (2013) Plant elicitor peptides are conserved signals regulating
810 direct and indirect antiherbivore defense. *Proc Natl Acad Sci USA* 110: 5707-5712
811 Hurst CH, Turnbull D, Myles SM, Leslie K, Keinath NF, Hemsley PA (2018) Variable effects
812 of C-terminal fusions on FLS2 function: not all epitope tags are created equal. *Plant*
813 *Physiol* 177: 522-531

814 Irani NG, Di Rubbo S, Mylle E, Van den Begin J, Schneider-Pizoń J, Hniliková J, Šiša M,
815 Buyst D, Vilarrasa-Blasi J, Szatmári A-M *et al* (2012) Fluorescent castasterone reveals
816 BRI1 signaling from the plasma membrane. *Nat Chem Biol* 8: 583-589
817 Irani NG, Di Rubbo S, Russinova E (2014) In vivo imaging of brassinosteroid endocytosis in
818 Arabidopsis. *Methods Mol Biol* 1209: 107-117
819 Jaillais Y, Vert G (2016) Brassinosteroid signaling and BRI1 dynamics went underground.
820 *Curr Opin Plant Biol* 33: 92-100
821 Kim SY, Xu Z-Y, Song K, Kim DH, Kang H, Reichardt I, Sohn EJ, Friml J, Juergens G,
822 Hwang I (2013) Adaptor protein complex 2–mediated endocytosis is crucial for male
823 reproductive organ development in *Arabidopsis*. *Plant Cell* 25: 2970-2985
824 Krol E, Mentzel T, Chinchilla D, Boller T, Felix G, Kemmerling B, Postel S, Arents M,
825 Jeworutzki E, Al-Rasheid KAS *et al* (2010) Perception of the *Arabidopsis* danger signal
826 peptide 1 involves the pattern recognition receptor *At*PEPR1 and its close homologue
827 *At*PEPR2. *J Biol Chem* 285: 13471-13479
828 Li B, Ferreira MA, Huang M, Camargos LF, Yu X, Teixeira RM, Carpinetti PA, Mendes GC,
829 Gouveia-Mageste BC, Liu C *et al* (2019) The receptor-like kinase NIK1 targets
830 FLS2/BAK1 immune complex and inversely modulates antiviral and antibacterial
831 immunity. *Nat Commun* 10: 4996
832 Lin W, Li B, Lu D, Chen S, Zhu N, He P, Shan L (2014) Tyrosine phosphorylation of protein
833 kinase complex BAK1/BIK1 mediates Arabidopsis innate immunity. *Proc Natl Acad Sci*
834 *USA* 111: 3632-3637
835 Liu D, Kumar R, Claus LAN, Johnson AJ, Siao W, Vanhoutte I, Wang P, Bender KW,
836 Yperman K, Martins S *et al* (2020) Endocytosis of BRASSINOSTEROID
837 INSENSITIVE1 is partly driven by a canonical Tyr-based motif. *Plant Cell* 32: 3598-
838 3612
839 Liu J, Chen S, Chen L, Zhou Q, Wang M, Feng D, Li J-F, Wang J, Wang H-B, Liu B (2017)
840 BIK1 cooperates with BAK1 to regulate constitutive immunity and cell death in
841 *Arabidopsis*. *J Integr Plant Biol* 59: 234-239
842 Liu Y, Huang X, Li M, He P, Zhang Y (2016) Loss-of-function of *Arabidopsis* receptor-like
843 kinase BIR1 activates cell death and defense responses mediated by BAK1 and SOBIR1.
844 *New Phytol* 212: 637-645
845 Liu Z, Wu Y, Yang F, Zhang Y, Chen S, Xie Q, Tian X, Zhou J-M (2013) BIK1 interacts
846 with PEPRs to mediate ethylene-induced immunity. *Proc Natl Acad Sci USA* 110: 6205-
847 6210

848 Lozano-Durán R, Macho AP, Boutrot F, Segonzac C, Somssich IE, Zipfel C (2013) The
849 transcriptional regulator BZR1 mediates trade-off between plant innate immunity and
850 growth. *eLife* 2: e00983
851 Lu D, Lin W, Gao X, Wu S, Cheng C, Avila J, Heese A, Devarenne TP, He P, Shan L (2011)
852 Direct ubiquitination of pattern recognition receptor FLS2 attenuates plant innate
853 immunity. *Science* 332: 1439-1442
854 Lu D, Wu S, Gao X, Zhang Y, Shan L, He P (2010) A receptor-like cytoplasmic kinase,
855 BIK1, associates with a flagellin receptor complex to initiate plant innate immunity. *Proc*
856 *Natl Acad Sci USA* 107: 496-501
857 Ma X, Claus LAN, Leslie ME, Tao K, Wu Z, Liu J, Yu X, Li B, Zhou J, Savatin DV *et al*
858 (2020) Ligand-induced monoubiquitination of BIK1 regulates plant immunity. *Nature*
859 581: 199-203
860 Martins S, Dohmann EMN, Cayrel A, Johnson A, Fischer W, Pojer F, Satiat-Jeunemaître B,
861 Jaillais Y, Chory J, Geldner N *et al* (2015) Internalization and vacuolar targeting of the
862 brassinosteroid hormone receptor BRI1 are regulated by ubiquitination. *Nat Commun* 6:
863 6151
864 Mbengue M, Bourdais G, Gervasi F, Beck M, Zhou J, Spallek T, Bartels S, Boller T, Ueda T,
865 Kuhn H *et al* (2016) Clathrin-dependent endocytosis is required for immunity mediated
866 by pattern recognition receptor kinases. *Proc Natl Acad Sci USA* 113: 11034-11039
867 Meng X, Chen X, Mang H, Liu C, Yu X, Gao X, Torii Keiko U, He P, Shan L (2015)
868 Differential function of *Arabidopsis* SERK family receptor-like kinases in stomatal
869 patterning. *Curr Biol* 25: 2361-2372
870 Mosesso N, Bläske T, Nagel M-K, Laumann M, Isono E (2019) Preparation of clathrin-coated
871 vesicles from *Arabidopsis thaliana* seedlings. *Front Plant Sci* 9: 1972
872 Mühlenbeck H, Tsutsui Y, Lemmon MA, Bender KW, Zipfel C (2024) Allosteric activation
873 of the co-receptor BAK1 by the EFR receptor kinase initiates immune signaling. *eLife* 12:
874 RP92110
875 Ntoukakis V, Schwessinger B, Segonzac C, Zipfel C (2011) Cautionary notes on the use of C-
876 terminal BAK1 fusion proteins for functional studies. *Plant Cell* 23: 3871-3878
877 Ortiz-Morea FA, Savatin DV, Dejonghe W, Kumar R, Luo Y, Adamowski M, Van den Begin
878 J, Dressano K, Pereira de Oliveira G, Zhao X *et al* (2016) Danger-associated peptide
879 signaling in *Arabidopsis* requires clathrin. *Proc Natl Acad Sci USA* 113: 11028-11033
880 Pavlos NJ, Friedman PA (2017) GPCR signaling and trafficking: The long and short of it.
881 *Trends Endocrinol Metab* 28: 213-226

882 Pei D, Hua D, Deng J, Wang Z, Song C, Wang Y, Wang Y, Qi J, Kollist H, Yang S *et al*
883 (2022) Phosphorylation of the plasma membrane H^+-ATPase AHA2 by BAK1 is required
884 for ABA-induced stomatal closure in Arabidopsis. *Plant Cell* 34: 2708-2729
885 Perraki A, DeFalco TA, Derbyshire P, Avila J, Séré D, Sklenar J, Qi X, Stransfeld L,
886 Schwessinger B, Kadota Y *et al* (2018) Phosphocode-dependent functional dichotomy of
887 a common co-receptor in plant signalling. *Nature* 561: 248-252
888 Robatzek S, Chinchilla D, Boller T (2006) Ligand-induced endocytosis of the pattern
889 recognition receptor FLS2 in *Arabidopsis*. *Genes Dev* 20: 537-542
890 Russinova E, Borst J-W, Kwaaitaal M, Caño-Delgado A, Yin Y, Chory J, de Vries SC (2004)
891 Heterodimerization and endocytosis of Arabidopsis brassinosteroid receptors BRI1 and
892 AtSERK3 (BAK1). *Plant Cell* 16: 3216-3229
893 Schulze B, Mentzel T, Jehle AK, Mueller K, Beeler S, Boller T, Felix G, Chinchilla D (2010)
894 Rapid heteromerization and phosphorylation of ligand-activated plant transmembrane
895 receptors and their associated kinase BAK1. *J Biol Chem* 285: 9444-9451
896 Schwessinger B, Roux M, Kadota Y, Ntoukakis V, Sklenar J, Jones A, Zipfel C (2011)
897 Phosphorylation-dependent differential regulation of plant growth, cell death, and innate
898 immunity by the regulatory receptor-like kinase BAK1. *PLoS Genet* 7: e1002046
899 Sigismund S, Confalonieri S, Ciliberto A, Polo S, Scita G, Di Fiore PP (2012) Endocytosis
900 and signaling: cell logistics shape the eukaryotic cell plan. *Physiol Rev* 92: 273-366
901 Song L, Shi Q-M, Yang X-H, Xu Z-H, Xue H-W (2009) Membrane steroid-binding protein 1
902 (MSBP1) negatively regulates brassinosteroid signaling by enhancing the endocytosis of
903 BAK1. *Cell Res* 19: 864-876
904 Takano J, Tanaka M, Toyoda A, Miwa K, Kasai K, Fuji K, Onouchi H, Naito S, Fujiwara T
905 (2010) Polar localization and degradation of *Arabidopsis* boron transporters through
906 distinct trafficking pathways. *Proc Natl Acad Sci USA* 107: 5220-5225
907 Tang J, Han Z, Sun Y, Zhang H, Gong X, Chai J (2015) Structural basis for recognition of an
908 endogenous peptide by the plant receptor kinase PEPR1. *Cell Res* 25: 110-120
909 Tunc-Ozdemir M, Li B, Jaiswal DK, Urano D, Jones AM, Torres MP (2017) Predicted
910 functional implications of phosphorylation of regulator of G protein signaling protein in
911 plants. *Front Plant Sci* 8: 1456
912 Vu LD, Xu X, Zhu T, Pan L, van Zanten M, de Jong D, Wang Y, Vanremoortele T, Locke
913 AM, van de Cotte B et al. (2021) The membrane-localized protein kinase
914 MAP4K4/TOT3 regulates thermomorphogenesis. *Nat Commun* 12: 2842.

915 Wang S, Yoshinari A, Shimada T, Hara-Nishimura I, Mitani-Ueno N, Feng Ma J, Naito S,
916 Takano J (2017) Polar localization of the NIP5;1 boric acid channel is maintained by
917 endocytosis and facilitates boron transport in Arabidopsis roots. *Plant Cell* 29: 824-842
918 Wang X, Kota U, He K, Blackburn K, Li J, Goshe MB, Huber SC, Clouse SD (2008)
919 Sequential transphosphorylation of the BRI1/BAK1 receptor kinase complex impacts
920 early events in brassinosteroid signaling. *Dev Cell* 15: 220-235
921 Wang Y, Li Z, Liu D, Xu J, Wei X, Yan L, Yang C, Lou Z, Shui W (2014) Assessment of
922 BAK1 activity in different plant receptor-like kinase complexes by quantitative profiling
923 of phosphorylation patterns. *J Proteomics* 108: 484-493
924 Wang Z-Y, Seto H, Fujioka S, Yoshida S, Chory J (2001) BRI1 is a critical component of a
925 plasma-membrane receptor for plant steroids. *Nature* 410: 380–383
926 Willems P, Sterck L, Dard A, Huang J, De Smet I, Gevaert K, Van Breusegem F (2024) The
927 Plant PTM Viewer 2.0: in-depth exploration of plant protein modification landscapes. *J*
928 *Exp Bot* 75: 4611-4624
929 Wiśniewska J, Xu J, Seifertová D, Brewer PB, Růžička K, Blilou I, Rouquié D, Benková E,
930 Scheres B, Friml J (2006) Polar PIN localization directs auxin flow in plants. *Science*
931 312: 883-883
932 Wu D, Liu Y, Xu F, Zhang Y (2018) Differential requirement of BAK1 C-terminal tail in
933 development and immunity. *J Integr Plant Biol* 60: 270-275
934 Yamada K, Yamashita-Yamada M, Hirase T, Fujiwara T, Tsuda K, Hiruma K, Saijo Y (2016)
935 Danger peptide receptor signaling in plants ensures basal immunity upon pathogen-
936 induced depletion of BAK1. *EMBO J* 35: 46-61
937 Yamaguchi Y, Huffaker A (2011) Endogenous peptide elicitors in higher plants. *Curr Opin*
938 *Plant Biol* 14: 351-357
939 Yamaguchi Y, Huffaker A, Bryan AC, Tax FE, Ryan CA (2010) PEPR2 is a second receptor
940 for the Pep1 and Pep2 peptides and contributes to defense responses in *Arabidopsis.*
941 *Plant Cell* 22: 508-522
942 Yin Y, Wang Z-Y, Mora-Garcia S, Li J, Yoshida S, Asami T, Chory J (2002) BES1
943 accumulates in the nucleus in response to brassinosteroids to regulate gene expression
944 and promote stem elongation. *Cell* 109: 181-191
945 Yu X, Xie Y, Luo D, Liu H, de Oliveira MVV, Qi P, Kim S-I, Ortiz-Morea FA, Liu J, Chen
946 Y *et al* (2023) A phospho-switch constrains BTL2-mediated phytocytokine signaling in
947 plant immunity. *Cell* 186: 2329-2344

948 Zhang J, Li W, Xiang T, Liu Z, Laluk K, Ding X, Zou Y, Gao M, Zhang X, Chen S *et al*
949 (2010) Receptor-like cytoplasmic kinases integrate signaling from multiple plant immune
950 receptors and are targeted by a *Pseudomonas syringae* effector. *Cell Host Microbe* 7:
951 290-301
952 Zhou J, Liu D, Wang P, Ma X, Lin W, Chen S, Mishev K, Lu D, Kumar R, Vanhoutte I *et al*
953 (2018) Regulation of *Arabidopsis* brassinosteroid receptor BRI1 endocytosis and
954 degradation by plant U-box PUB12/PUB13-mediated ubiquitination. *Proc Natl Acad Sci*
955 *USA* 115: E1906-E1915
956

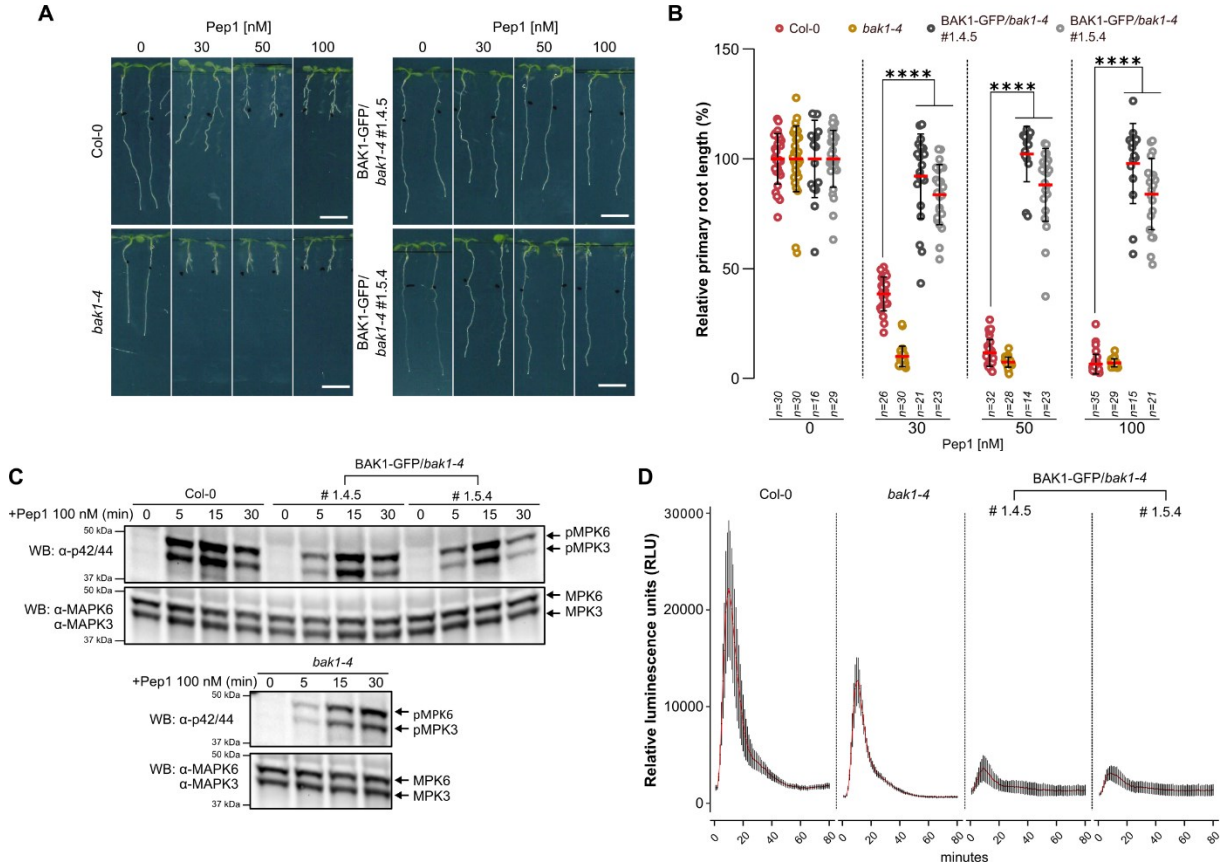

Figure 1. C-terminally tagged BAK1-GFP is not fully functional in Pep1-induced immune responses.

(A) Representative images of root growth inhibition caused by different Pep1 concentrations. Seedlings of wild-type Col-0, *bak1-4*, and two independent *pBAK1-BAK1-GFP*/*bak1-4* transgenic lines (#1.4.5 and #1.5.4) were grown for 4 days on ½MS agar medium and transferred to ½MS agar medium supplemented with different concentrations of Pep1 or water (mock) for a further 3 days. Scale bars, 10 mm.

(B) Primary root length of seedlings in **(A)** presented as relative to the mock-treated control for each genotype. Individual measurements, average, and SD are represented by dots, red lines, and whiskers, respectively. Two-way ANOVA followed by Tukey's test was used to determine significant differences.****$P<0.0001$; *n*, number of seedlings analyzed.

(C) MAPK activation assay of seven-day-old seedlings in **(A)** treated with 100 nM Pep1 for the indicated time points. Phosphorylated MPK3 (pMPK3) and MPK6 (pMPK6) were detected by Western Blotting (WB) with α-p42/44 antibody (top). Protein loading is shown by total MPK3 and MPK6 detected with α-MPK3 and α-MPK6 antibodies (bottom).

(D) Pep1-induced reactive oxygen species (ROS) production. Eight leaf discs from four 5-week-old plants in (A) treated with 100 nM of Pep1. ROS production measured as RLU was detected at the indicated time points. Red lines indicate means ± SD.

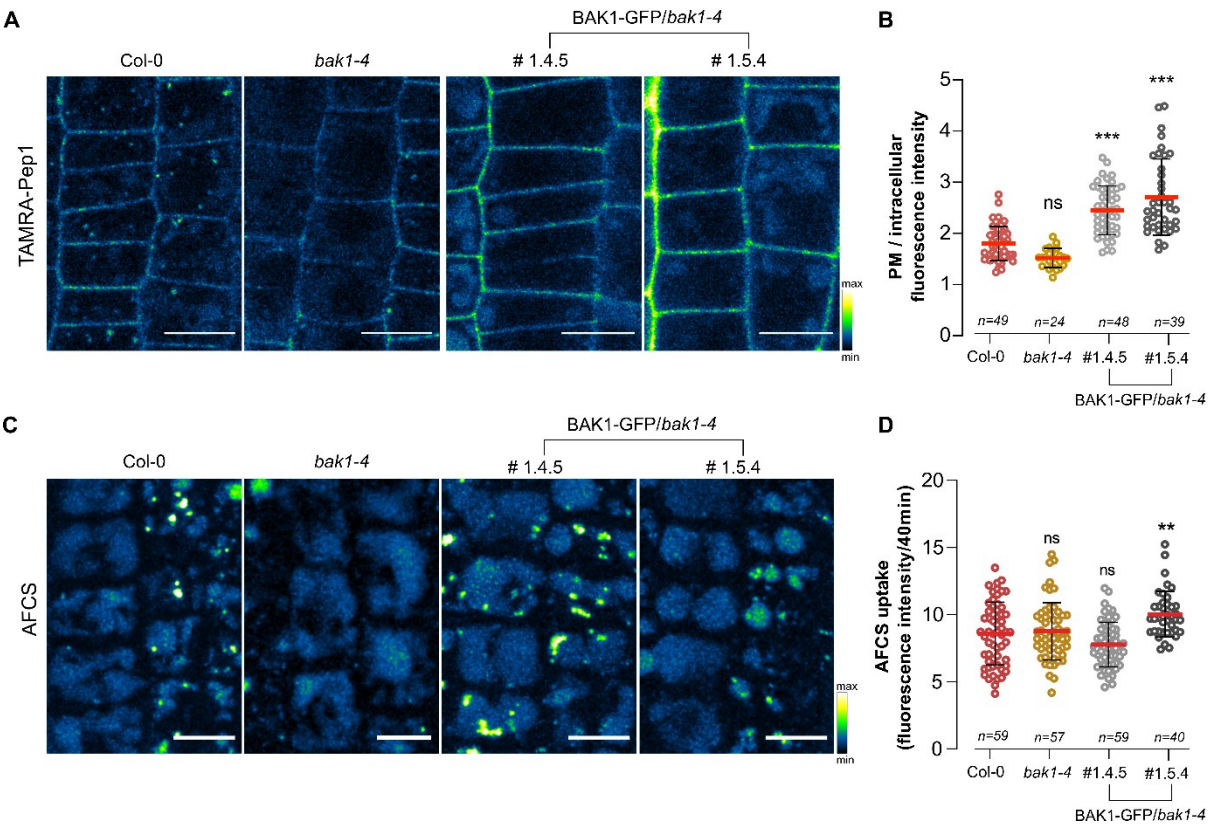

Figure 2. Pep1-triggered PEPR1 endocytosis requires functional BAK1.

(A, C) Representative images of TAMRA-Pep1 **(A)** and AFCS **(C)** root uptake visualized by color-based fluorescence intensity coding. Five-day-old seedlings of wild-type Col-0, *bak1-4*, and two independent *pBAK1-BAK1-GFP*/*bak1-4* transgenic lines were treated with 100 nM TAMRA-Pep1 for 10 s (pulse) and with 40 µM AFCS for 20 min (pulse), respectively, and imaged after 40 min (chase). Epidermal cells of root meristematic zone were imaged. Scale bars, 10 µm.

(B, D) Fluorescence intensity measurements of plasma membrane (PM) vs intracellular compartments of the **(B)** TAMRA-Pep1 uptake in **(A)** and **(D)** the AFCS uptake after 40 min chase in **(C)**. Individual measurements, average, and SD are represented by dots, red line, and whiskers, respectively. One-way ANOVA followed by Tukey's test was used to determine significant differences.***$P<0.001$, **$P<0.01$; *n*, number of cell analyzed; ns, not significant.

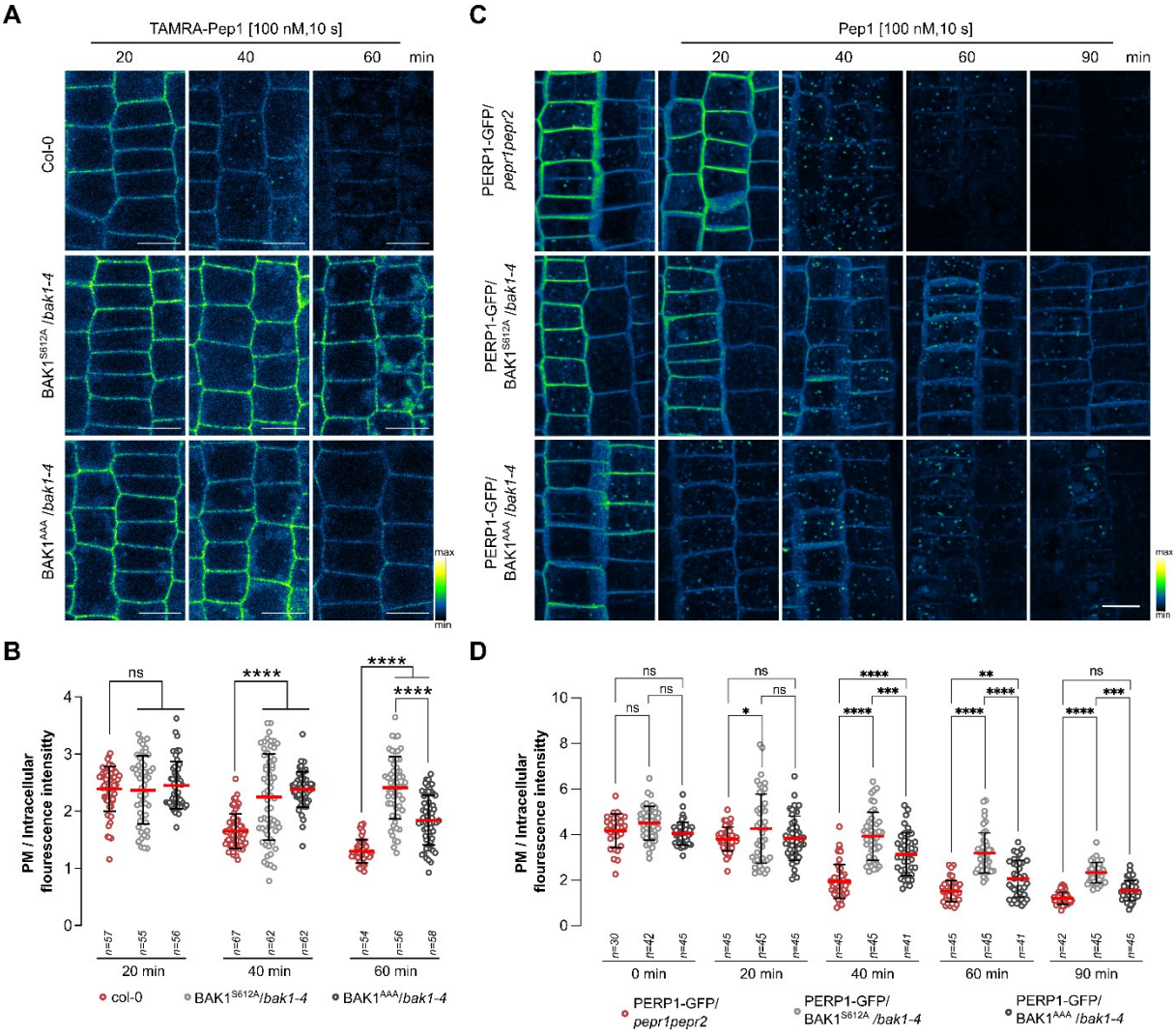

Figure 3. The BAK1 phosphorylation essential for flagellin-induced signaling influences PEPR1 endocytosis.

(A) Representative images of TAMRA-Pep1 root uptake visualized by color-based fluorescence intensity coding. Five-day-old wild-type Col-0, *pBAK1-BAK1^{S612A}/bak1-4* and *pBAK1-BAK1^{AAA}/bak1-4* seedlings were treated with 100 nM TAMRA-Pep1 for 10 s (pulse) and imaged at indicated time points (chase). Epidermal cells of root meristematic zone were imaged. Scale bars, 10 µm.

(B) Plasma membrane (PM) vs. intracellular fluorescence intensity measurements of the TAMRA-Pep1 uptake in **(A)**. Individual measurements, average, and SD are indicated as dots, red line, and whiskers, respectively. One-way ANOVA followed by Tukey's test was used to determine significant differences.****P<0.0001.

(C) Representative images of PEPR1-GFP endocytosis visualized by color-based fluorescence intensity coding. Five-day-old *pRPS5A-PEPR1-GFP/pepr1pepr2*, *pRPS5A-PEPR1-GFP/pBAK1-BAK1^{S612A}/bak1-4* and *pRPS5A-PEPR1-GFP/pBAK1-BAK1^{AAA}/bak1-4* seedlings

1004 were treated with 100 nM Pep1 for 10 s (pulse) and imaged at indicated time points (chase).
1005 Images are a maximum intensity Z-projection. Epidermal cells of root meristematic zone were
1006 imaged. Scale bar, 10 µm.
1007 **(D)** PM vs. intracellular fluorescence intensity measurements of PEPR1-GFP internalization in
1008 **(C)**. Dots, red lines, and whiskers represent individual measurements, red lines, and SD,
1009 respectively. One-way ANOVA followed by Tukey's test was used to determine significant
1010 differences.****P<0.0001, ***P<0.001, **P<0.01, *P<0.05; n, number of cell analyzed **(B,**
1011 **D)**; ns, not significant.

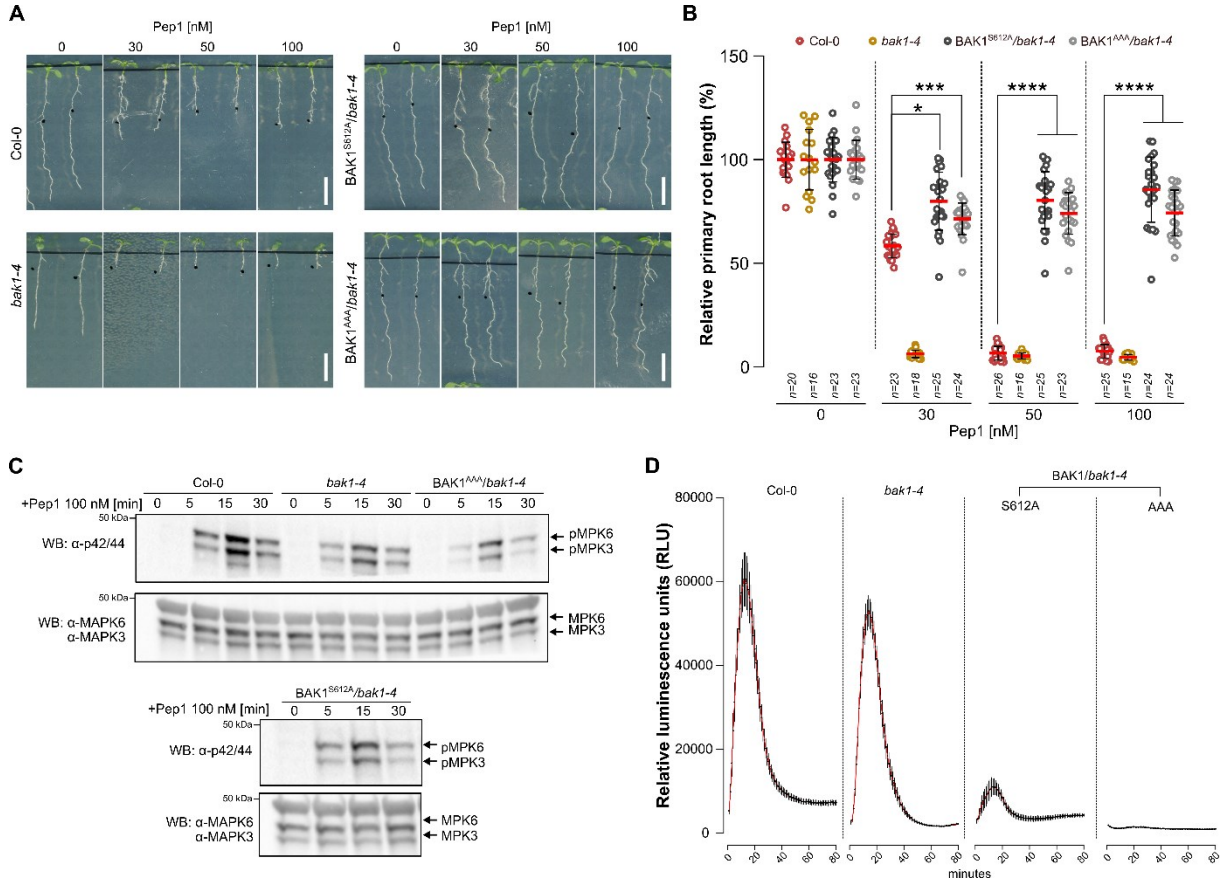

Figure 4. Flagellin-and Pep1-induced signaling pathways require the same BAK1 phosphorylation signature.

(A) Representative images of root growth inhibition caused by different Pep1 concentrations. Seedlings of wild-type Col-0, *bak1-4*, *pBAK1-BAK1^{S612A}/bak1-4* and *pBAK1-BAK1^{AAA}/bak1-4* were grown for 4 days on ½MS agar plates and transferred to ½MS solid media supplemented with different concentrations of Pep1 or water (mock) for a further 3 days. Scale bars, 10 mm.

(B) Primary root length of seedlings in **(A)** presented as relative to the mock-treated control for each genotype. Dots, red lines, and whiskers represent individual measurements, averages, and SD, respectively. The asterisk indicates statistically significant difference analyzed with two-way ANOVA followed by Tukey's test. ****P<0.0001, ***P<0.001, *P<0.05; n, number of seedlings analyzed; ns, not significant.

(C) MAPK activation assay of 5-day-old seedlings in **(A)** treated with 100 nM Pep1 for the indicated time points. Phosphorylated MPK3 (pMPK3) and MPK6 (pMPK6) were detected by Western Blotting (WB) with the α-p42/44 antibody (top). Protein loading is shown by total MPK3 and MPK6 detected with the α-MPK3 and α-MPK6 antibodies (bottom).

(D) Pep1-induced reactive oxygen species (ROS) production. Eight leaf discs from four 5-week-old plants in **(A)** were treated with 100 nM of Pep1. ROS production measured as RLU was detected at the indicated time points. Red lines indicate means ± SD.

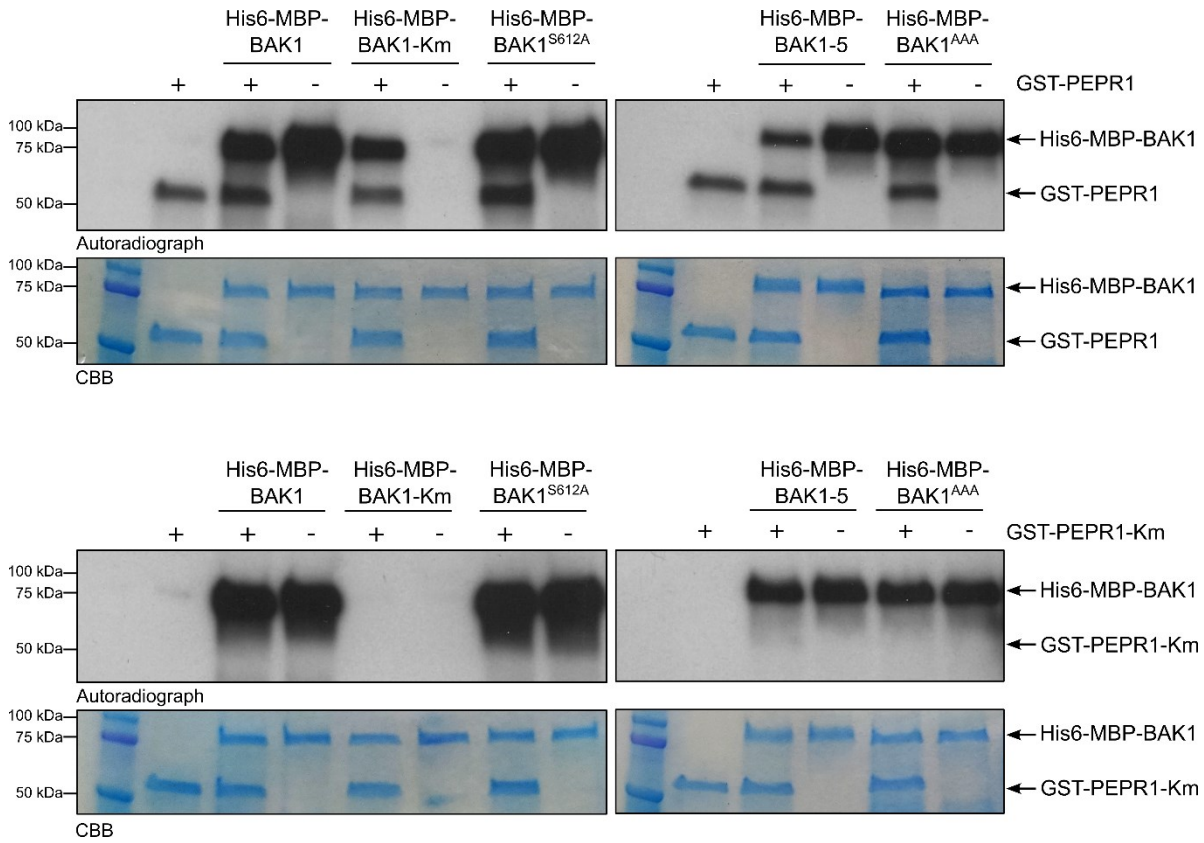

Figure 5. BAK1 cannot trans-phosphorylate PEPR1 *in vitro.*

The cytoplasmic domains of BAK1^{S612A}, BAK1^{AAA}, BAK1-5, BAK1, and PEPR1, and their respective kinase-dead mutant (Km) versions of PEPR1-Km (K855E) and BAK1-Km (D416N) tagged with either glutathione S-transferase (GST) or His6-maltose-binding protein (MBP) were produced in bacteria. *In vitro* kinase assay performed with a single or combined recombinant proteins as indicated. CBB, Coomassie Brilliant Blue.

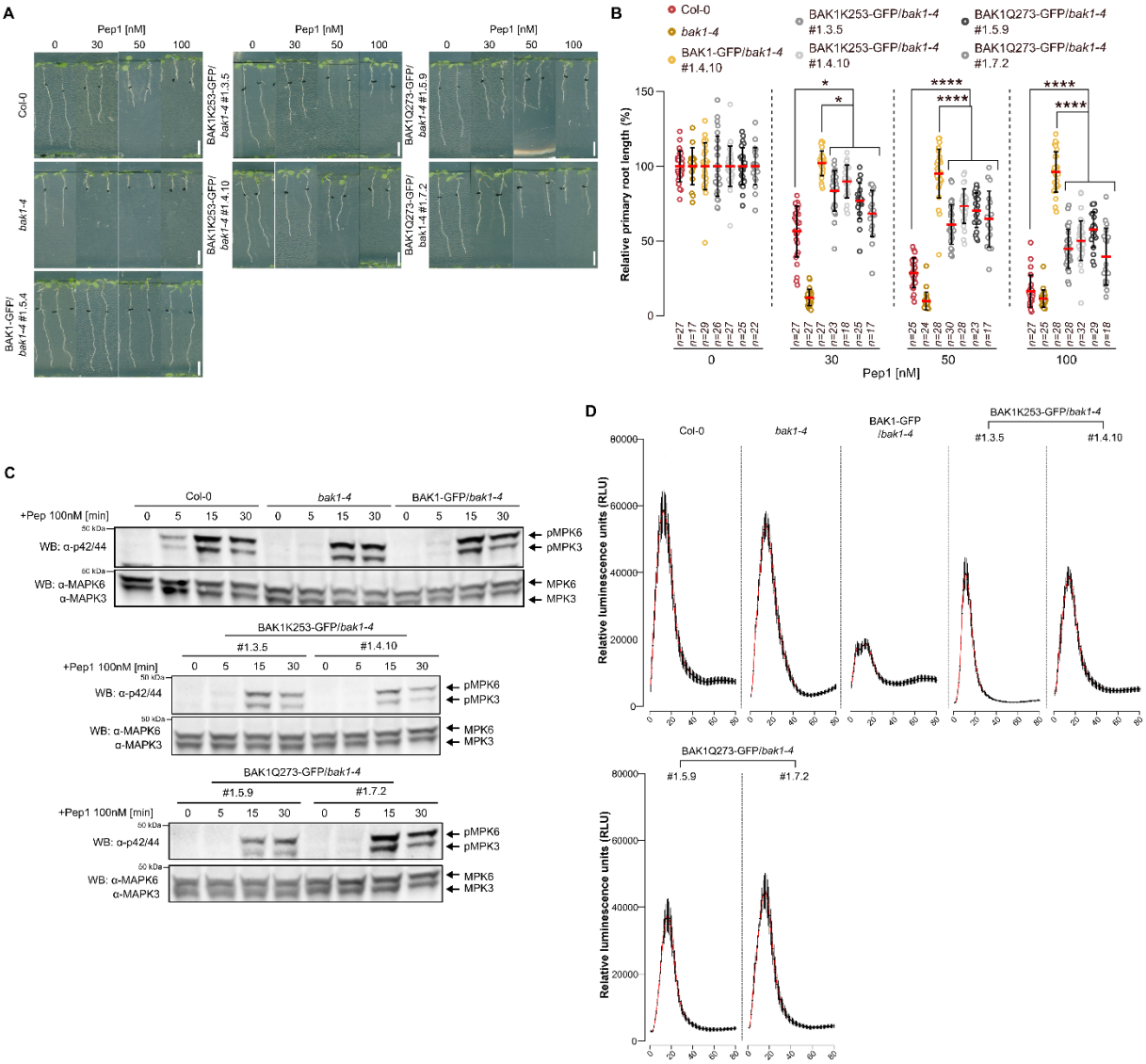

Figure 6. Arabidopsis plants expressing BAK1K253-GFP and BAK1Q273-GFP are partially sensitive to exogenous Pep1.

(A) Representative images of root growth inhibition caused by different Pep1 concentrations. Seedlings of wild-type Col-0, *bak1-4*, *pBAK1-BAK1-GFP/bak1-4*, and two independent transgenic lines of each *pBAK1-BAK1K253-GFP/bak1-4* and *pBAK1-BAK1Q273-GFP/bak1-4* were grown for 4 days on ½MS agar plates and then transferred to a ½MS solid media supplemented with different concentrations of Pep1 or water (mock) for a further 3 days. Scale bars, 10 mm.

(B) Primary root length of seedlings in **(A)** presented as relative to the mock-treated control for each genotype. Dots, red lines, and whiskers represent individual measurements, averages, and SD. Statistically significant difference analyzed with two-way ANOVA followed by Tukey's test; ****P<0.0001, *P<0.05; n, number of seedlings analyzed.

1051 **(C)** MAPK activation assay after Pep1 application of 5-day-old seedlings as in **(A)** treated with
1052 100 nM Pep1 for the indicated time points. Phosphorylated MPK3 (pMPK3) and MPK6
1053 (pMPK6) were detected by Western Blotting (WB) with the α-p42/44 antibody (top). Protein
1054 loading is shown by total MPK3 and MPK6 detected with the α-MPK3 and α-MPK6 antibodies
1055 (bottom).
1056 **(D)** Pep1-induced reactive oxygen species (ROS) production. Eight leaf discs from four 5-
1057 week-old plants in (A) were treated with 100 nM of Pep1. ROS production measured as RLU
1058 was detected at the indicated time points. Red lines indicate mean ± SD.
1059

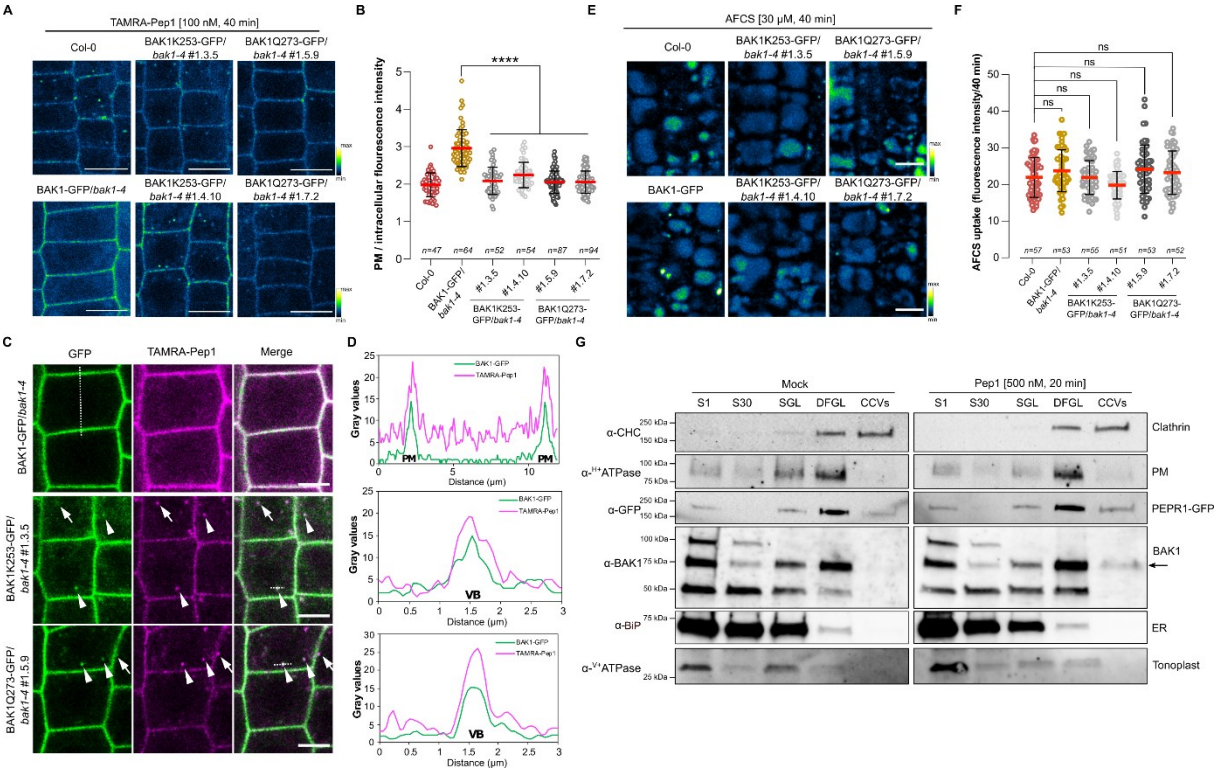

Figure 7. BAK1 and PEPR1 are likely co-internalized.

(A, E) Representative images of TAMRA-Pep1 **(A)** and AFCS **(E)** root uptake visualized by color-based fluorescence intensity coding. Five-day-old seedlings of wild-type Col-0, *bak1-4*, *pBAK1-BAK1-GFP/bak1-4*, *pBAK1-BAK1K253-GFP/bak1-4* and *pBAK1-BAK1Q273-GFP/bak1-4* were treated with 100 nM TAMRA-Pep1 for 10 s (pulse) and with 40 μM of AFCS for 20 min (pulse), respectively, and imaged after 40 min (chase). Epidermal cells of root meristematic zone were imaged. Scale bars, 10 μm.

(B, F) Fluorescence intensity measurements of the plasma membrane (PM) vs. intracellular compartments of the TAMRA-Pep1 uptake in **(A)** and AFCS uptake **(E)** after 40 min chase. Dots, red lines, and whiskers represent individual measurements, averages, and SD. The one-way ANOVA followed by Tukey's test was used to determine significant differences. ****$P<0.0001$; ns, not significant; *n*, number of cell analyzed.

(C) Co-localization of BAK1-GFP and TAMRA-Pep1. Five-day-old *pBAK1-BAK1-GFP/bak1-4*, *pBAK1-BAK1K253-GFP/bak1-4* and *pBAK1-BAK1Q273-GFP/bak1-4* seedlings were treated with 100 nM of TAMRA-Pep1 for 10 s (pulse) and imaged after 40 min (chase). Arrowheads and arrows indicate co-localizing puncta and TAMRA-Pep1 puncta only, respectively. Scale bars, 10 μm.

1078 **(D)** Line plot of the BAK1-GFP and TAMRA-Pep1 fluorescent signals of the dashed line in
1079 **(C)** VB, vesicle body; PM, plasma membrane. Epidermal cells of root meristematic zone were
1080 imaged.
1081 **(G)** Co-localization between PEPR1 and BAK1 in clathrin-coated vesicles (CCVs). CCVs were
1082 prepared from total plant extracts of 10-day-old *pRPS5A-PEPR1-GFP/pepr1pepr2* seedlings.
1083 Samples were collected during CCV purification and subjected to Western Blotting (WB) with
1084 antibodies against clathrin heavy chain (CHC), GFP, BAK1, and various subcellular organelle
1085 marker proteins. S1, supernatant after centrifugation at 1000*g*; S30, supernatant after
1086 centrifugation at 30,000*g*; SGL, sucrose step gradient load; DFGL, deuterium oxide/ficoll
1087 gradient load; CCVs, CCV-containing fraction. The following antibodies were used as
1088 organelle- or compartment-specific markers: α-H-ATPase (PM), α-V-ATPase (vacuole), and
1089 α-BiP (ER; endoplasmic reticulum).
1090

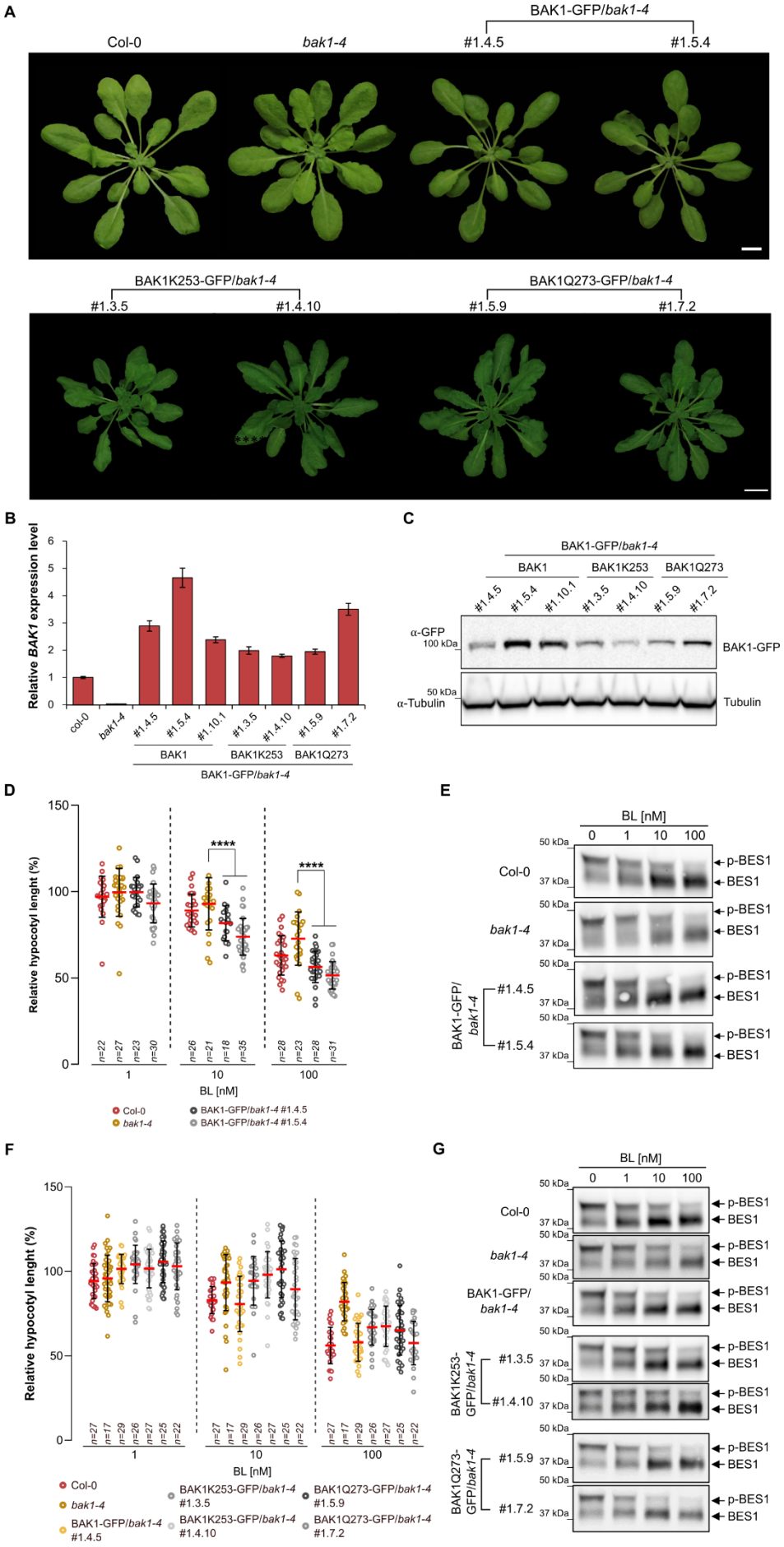
A
BAK1-GFP/bak1-4
Col-0
bak1-4
#1.4.5
#1.5.4
BAK1K253-GFP/bak1-4
#1.3.5
#1.4.10
BAK1Q273-GFP/bak1-4
#1.5.9
#1.7.2
B
Relative BAK1 expression level
col-0
bak1-4
BAK1
BAK1K253
BAK1Q273
BAK1-GFP/bak1-4
C
α-GFP
100 kDa
BAK1-GFP
50 kDa
α-Tubulin
Tubulin
D
Relative hypocotyl lenght (%)
BL [nM]
Col-0
bak1-4
BAK1-GFP/bak1-4 #1.4.5
BAK1-GFP/bak1-4 #1.5.4
E
BL [nM]
p-BES1
BES1
F
BAK1K253-GFP/bak1-4 #1.3.5
BAK1K253-GFP/bak1-4 #1.4.10
BAK1Q273-GFP/bak1-4 #1.5.9
BAK1Q273-GFP/bak1-4 #1.7.2
G

1091

1092 **Supplemental Figure 1. The C-terminal BAK1-GFP tag did not impair BR responses.**
1093 **(A)** Representative images of 4-week-old plants of the indicated genotypes. Scale bars, 1 cm.
1094 **(B)** Real-time quantitative reverse transcription PCR (qRT-PCR) analysis of *BAK1*. Total RNA
1095 was isolated from 7-day-old seedlings of two or three independent transgenic lines. Transcript
1096 levels were normalized to *GAPDH* and *ACTIN2* gene expression and three biological with three
1097 technical replicates each were quantified. Data are means ± SD.
1098 **(C)** Total proteins isolated from 7-day-old seedlings and detected by Western Blotting (WB)
1099 with α-GFP antibodies to detect the BAK1-GFP. Numbers indicate individual transgenic lines.
1100 α-tubulin antibodies were used to equilibrate protein loading.
1101 **(D, F)** Hypocotyl length measurements after brassinolide (BL) treatment relative to the mock
1102 (DMSO). Seedlings of wild-type Col-0, *bak1-4* and two independent transgenic lines of each
1103 *pBAK1-BAK1-GFP*/*bak1-4*, *pBAK1-BAK1K253-GFP*/*bak1-4,* and *pBAK1-BAK1Q273-*
1104 *GFP*/*bak1-4* were grown for 4 days in the dark on ½MS agar plates supplemented with
1105 increasing concentrations of BL. Dots, red lines, and whiskers represent individual
1106 measurements, averages, and SD, respectively. Statistically significant difference were
1107 analyzed with two-way ANOVA followed by a Tukey's test. ****P<0.0001; n, number of
1108 seedlings analyzed.
1109 **(E, G)** BES1 dephosphorylation assay after BL treatment. Five-day-old seedlings of wild-type
1110 Col-0, *bak1-4* and of two independent transgenic lines of each *pBAK1-BAK1-GFP*/*bak1-4*,
1111 *pBAK1-BAK1K253-GFP*/*bak1-4,* and *pBAK1-BAK1Q273-GFP*/*bak1-4* were treated with
1112 increasing concentrations of BL for 1 h. BES1 was detected by WB with the α-BES1 antibody
1113 and discrimination between phosphorylated (p-BES1) and unphosphorylated BES1 was based
1114 on the protein size shift.
1115

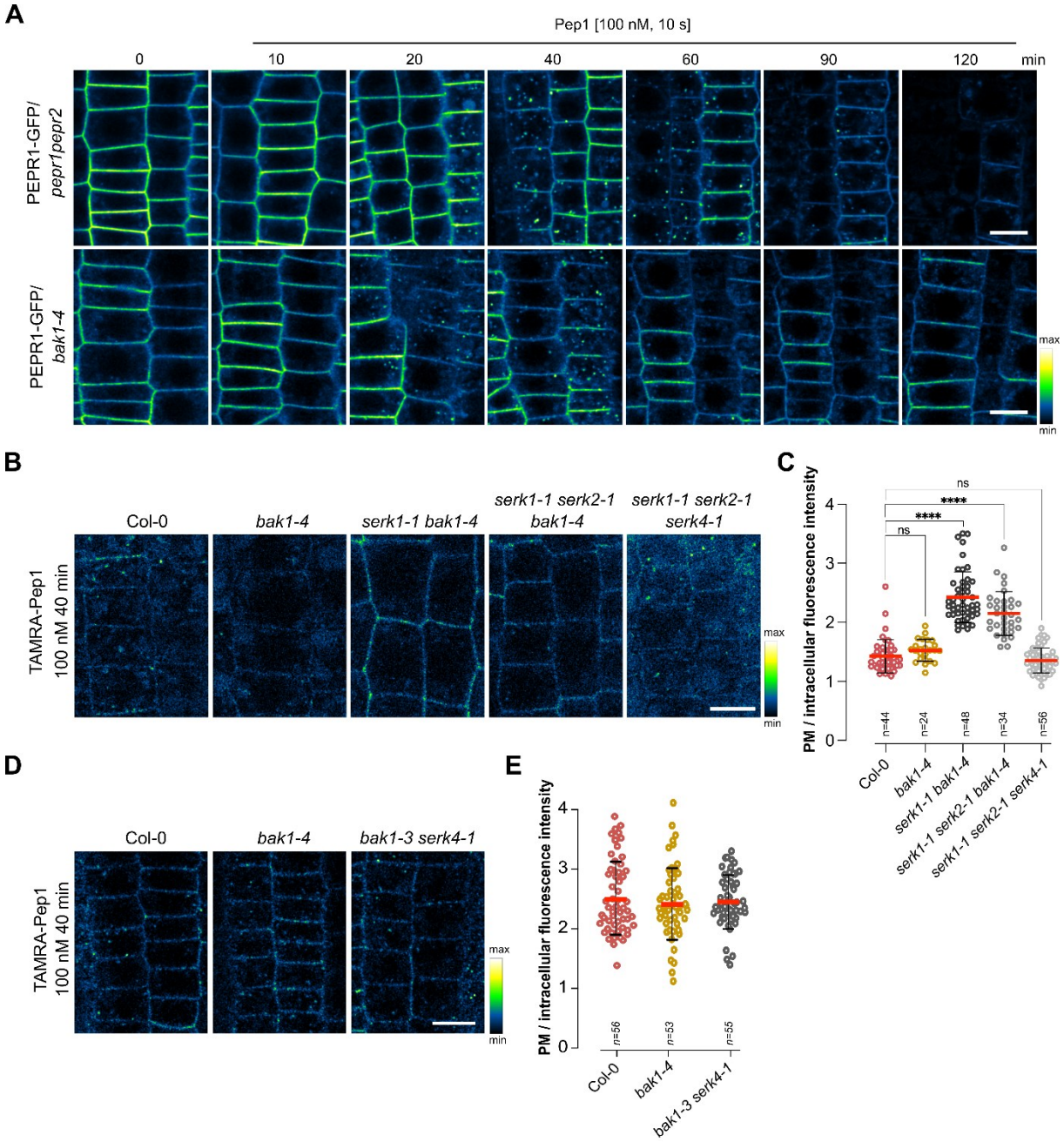

Supplemental Figure 2. PEPR1 endocytosis requires SERKs.

(A) Representative images of PEPR1-GFP endocytosis in roots of *pepr1pepr2* and *bak1-4* mutants. Five-day-old *pRPS5A-PEPR1-GFP/pepr1pepr2* and *pRPS5A-PEPR1-GFP/bak1-4* seedlings were treated with 100 nM Pep1 for 10 s (pulse) and imaged at the indicated time points (chase).

(**B, D**) TAMRA-Pep1 root uptake visualized by color-based fluorescence intensity coding. 5-day-old wild-type Col-0*, bak1-4, serk1-1bak1-4*, *serk1-1serk2-1bak1-4* and *serk1-1serk2-1serk4-1* (**B**) and Col-0, *bak1-4* and *bak1-3serk4-1* (**D**) seedlings were treated with 100 nM of TAMRA-Pep1 for 10 s (pulse) and imaged after 40 min (chase). Homozygous seedlings for the triple mutants were selected based on phenotype.

1127 **(C, E)** Plasma membrane (PM) vs. intracellular fluorescence intensity measurements of the
1128 TAMRA-Pep1 uptake in **(B, D)**. Dots, red lines, and whiskers represent individual
1129 measurements, averages, and SD, respectively. Statistically significant differences were
1130 analyzed with one-way ANOVA followed by Tukey's test. ****P<0.0001; ns, not significant;
1131 n, number of cell analyzed. Epidermal cells of root meristematic zone were imaged (**A, B, D**).
1132 Scale bars, 10 µm (**A, B, D**).

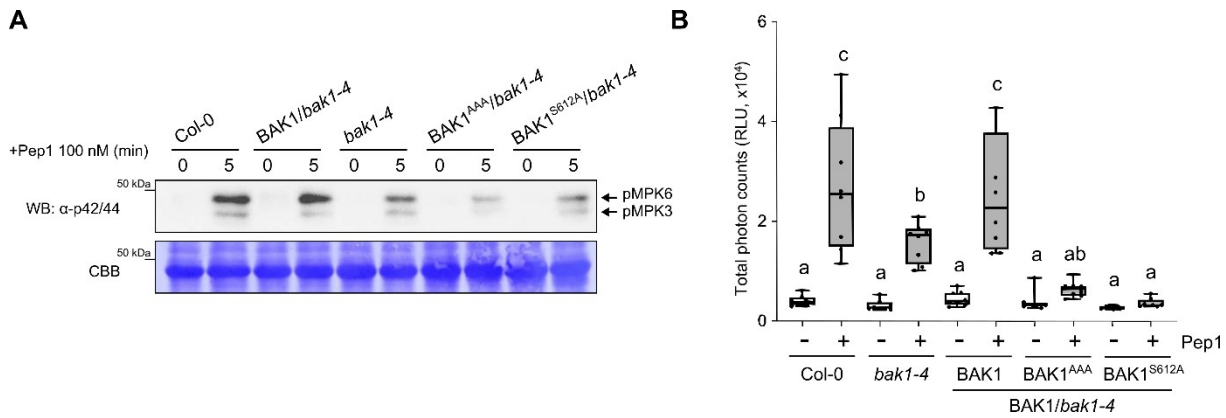

Supplemental Figure 3. MAPK activation and ROS burst after Pep1 treatment were impaired in the BAK1^{S612A} and BAK1^{AAA} mutants

(**A**) Pep1-mediated MAPK activation was compromised in BAK1^{S612A} and BAK1^{AAA} mutants as shown in *bak1-4* mutant. 9-day-old seedlings of wild-type (Col-0), *pBAK1-BAK1*/*bak1-4*, *pBAK1-BAK1^{S612A}*/*bak1-4*, and *pBAK1-BAK1^{AAA}*/*bak1-4* were treated with 100 nM Pep1 and with mock (water) for 5 min. MAPK activation was analyzed with α-pERK1/2 antibodies (top), and protein loading is shown by CBB staining for RBC (bottom).

(**B**) The BAK1^{S612A} and BAK1^{AAA} mutants showed compromised Pep1-induced ROS burst. Leaf discs (n = 8) from 4-week-old soil-grown plants were treated with or without 300 nM Pep1, and ROS production was measured as relative light units (RLUs) by a luminometer. Data represent mean ± SEM

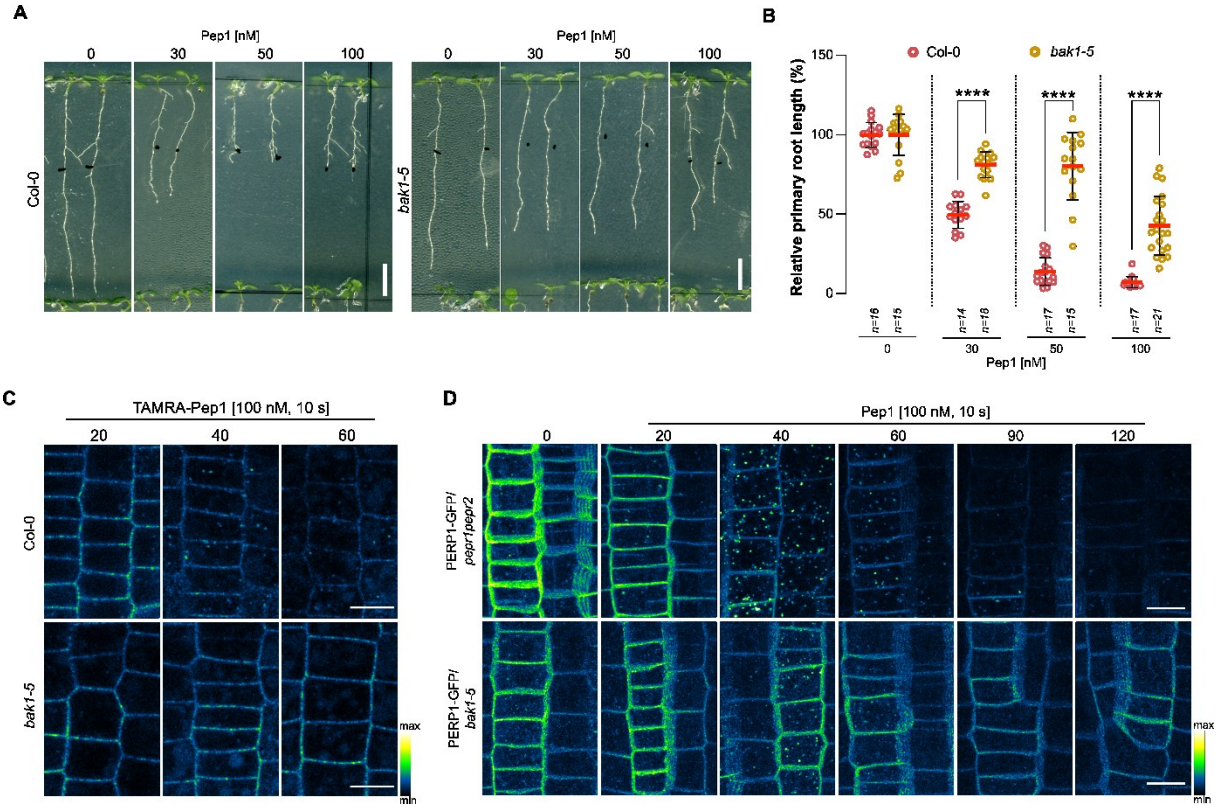

Supplemental Figure 4. The hypoactive kinase BAK1-5 disrupts PEPR1 endocytosis and signaling.

(A) Representative images of the root growth inhibition caused by different Pep1 concentrations. Seedlings of wild-type Col-0 and *bak1-5* were grown for 4 days on ½MS agar plates and transferred to ½MS agar media supplemented with different concentrations of Pep1 or water (mock) for 3 days. Scale bars, 10 mm.

(B) Primary root length of seedlings in **(A)** presented as relative to the mock-treated control for each genotype. Dots, red lines, and whiskers represent individual measurements, averages, and SD, respectively. The two-way ANOVA followed by Tukey's test was used to determine significant differences. ****P<0.0001; n, number of seedlings analyzed.

(C, D) Representative images of TAMRA-Pep1 root uptake **(C)** and PEPR1-GFP endocytosis **(D)** in the *bak1-5* mutant visualized by color-based fluorescence intensity coding. Five-day-old seedlings of wild-type Col-0 and *bak1-5* **(C)**, and *pRPS5A-PEPR1-GFP*/*pepr1pepr2* and *pRPS5A-PEPR1-GFP*/*bak1-5* were treated with 100 nM of TAMRA-Pep1 **(C)** and 100 nM Pep1 **(D)** for 10 s and imaged at indicated time points (chase). Epidermal cells of root meristematic zone were imaged. Images are maximum intensity Z-projections. Scale bars, 10 µm.

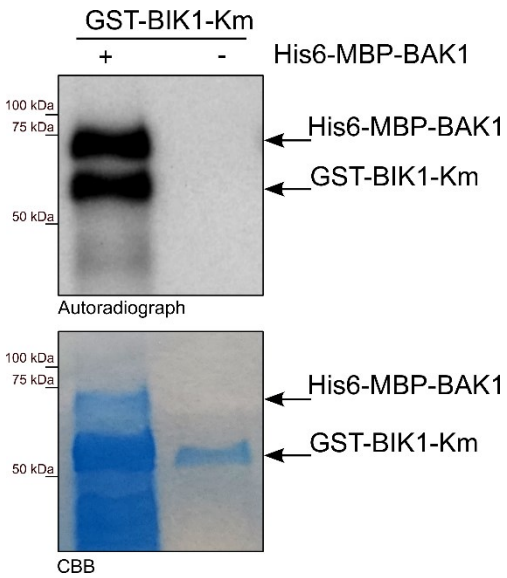

Supplemental Figure 5. His6-MBP-BAK1 can phosphorylate the inactive BIK1 kinase (BIK1-Km).

For the *in vitro* kinase assay a single or recombinant proteins together were used, as indicated. Protein loading was controlled by Coomassie Brilliant Blue (CBB).

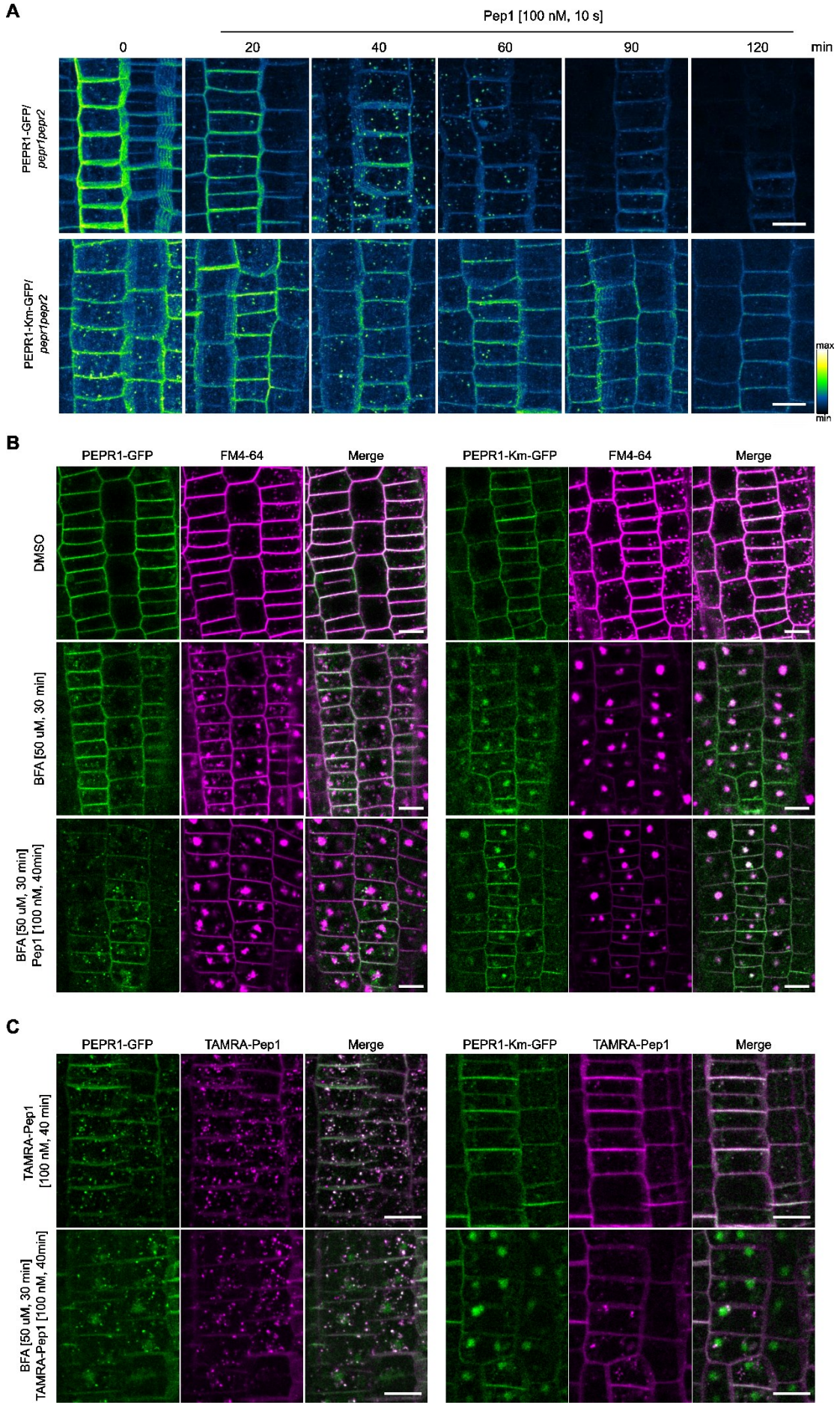
A
Pep1 [100 nM, 10 s]
0
20
40
60
90
120
min
PEPR1-GFP/
pepr1pepr2
PEPR1-Km-GFP/
pepr1pepr2
max
min
B
PEPR1-GFP
FM4-64
Merge
PEPR1-Km-GFP
FM4-64
Merge
DMSO
BFA [50 uM, 30 min]
BFA [50 uM, 30 min]
Pep1 [100 nM, 40min]
C
PEPR1-GFP
TAMRA-Pep1
Merge
PEPR1-Km-GFP
TAMRA-Pep1
Merge
TAMRA-Pep1
[100 nM, 40 min]
BFA [50 uM, 30 min]
TAMRA-Pep1 [100 nM, 40min]

1169

1170 **Supplemental Figure 6. The kinase activity of PEPR1 is required for its endocytosis.**
1171 **(A)** Representative images of PEPR-GFP and PEPR1-Km-GFP (PEPR1-kinase mutant- GFP)
1172 internalization visualized by color-based fluorescence intensity coding. Five-day-old *pRPS5A-*
1173 *PEPR1-GFP/pepr1pepr2* and *pRPS5A-PEPR1-Km-GFP/pepr1pepr2* seedlings were treated
1174 with 100 nM of Pep1 for 10 s (pulse) and imaged at the indicated time points (chase). Epidermal
1175 cells of root meristematic zone were imaged. Images are maximum intensity Z-projections.
1176 Scale bars, 10 µm.
1177 **(B, C)** Representative images of PEPR1-GFP/*pepr1pepr2* and PEPR1-Km-GFP/*pepr1pepr2*
1178 internalization in the presence of BFA **(B)** and endocytosis of TAMRA-Pep1 in the absence
1179 and presence of BFA **(C)**. Seedlings as in **(A)** were treated with DMSO (mock), BFA (50 µM,
1180 30 min) and Pep1 (100 nM, 40 min) after pre-treatment with BFA (50 µM, 30 min) **(B)**.
1181 Seedlings as in **(A)** were treated with TAMRA-Pep1 (100 nM, 40 min) or TAMRA-Pep1
1182 (100 nM, 40 min) after pre-treatment with BFA (50 µM, 30 min) **(C)**. Epidermal cells of the
1183 root meristematic zone were imaged. Images are maximum Z-projections. 2 µM FM64 (*N*-(3-
1184 triethylammoniumpropyl)-4-(6-(4-(diethylamino) phenyl) hexatrienyl) pyridinium dibromide)
1185 dye was used to visualize general endocytosis in **(B)**. Scale bars, 10 µm.
1186

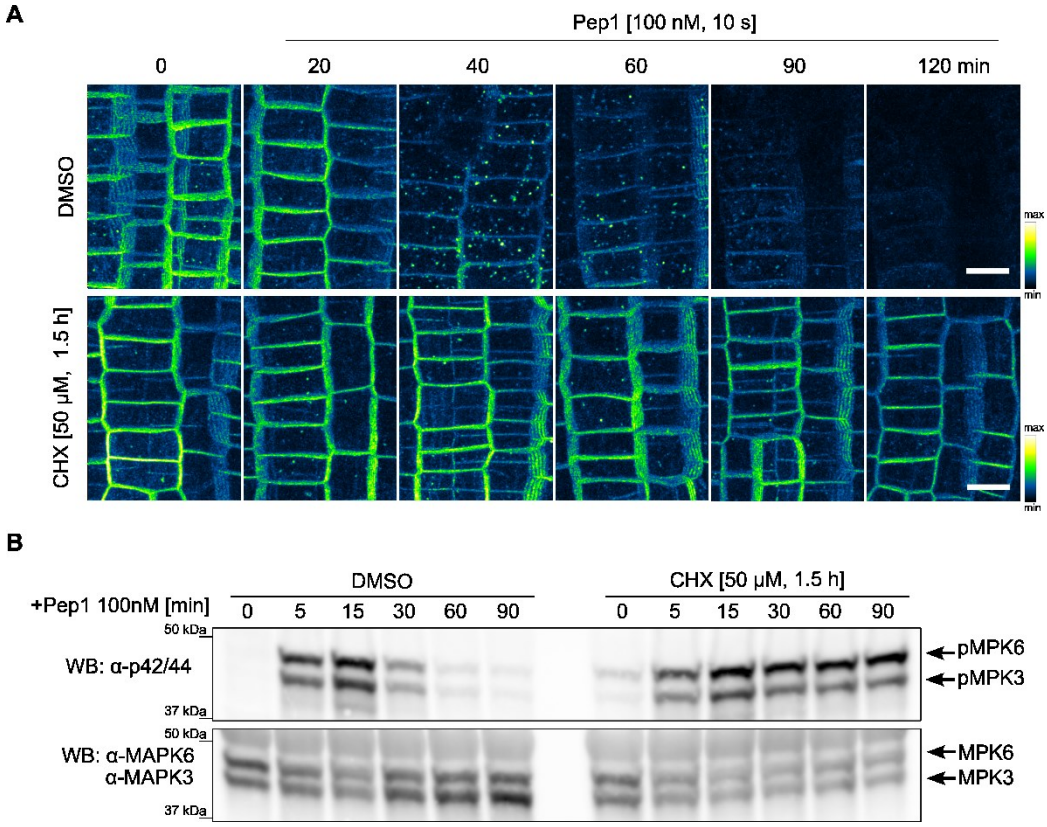

Supplemental Figure 7. Cycloheximide (CHX) blocks PEPR1-GFP endocytosis and affects Pep1-triggered MAPK activation

(A) Representative images of PEPR1-GFP internalization visualized by color-based fluorescence intensity coding in the presence of CHX. Five-day-old *pRPS5A-PEPR1-GFP/pepr1pepr2* seedlings were pre-treated with DMSO (mock) and CHX (50 µM, 1.5 h) followed by application of 100 nM Pep1 for 10 s (pulse) and imaged at the indicated time points (chase). Epidermal cells of root meristematic zone were imaged. Images are maximum intensity Z-projections. Scale bars, 10 µm.

(B) MAPK activation assay after Pep1 treatment in the presence of CHX. Five-day-old wild-type Col-0 seedlings were pre-treated with DMSO (mock) or CHX (50 µM, 1.5 h) followed by application of 100 nM Pep1 for the indicated time points. Phosphorylated MPK3 (pMPK3) and MPK6 (pMPK6) were detected by Western Blotting (WB) with α-p42/44 antibody (top). Protein loading of total MPK3 and MPK6 was detected with the α-MPK3 and α-MPK6 antibodies (bottom).

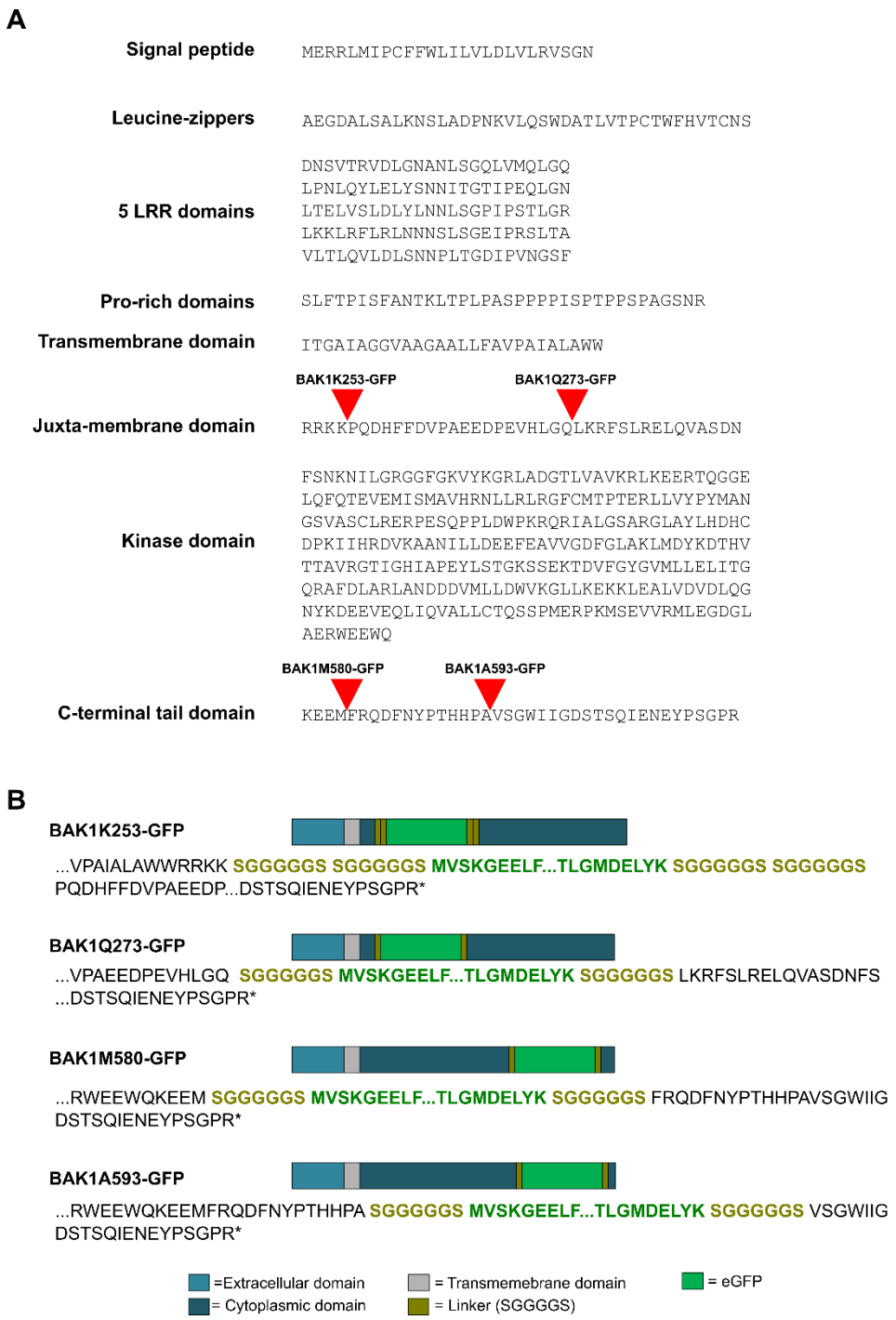

Supplemental Figure 8. Schematic representation of the different constructs containing GFP-tagged BAK1.

(A) Amino acid sequences of the different BAK1 protein domains. The positions of the GFP tags are indicated with red triangle. LRR, leucine-rich repeat.

(B) Schematic representation of the tagged BAK1-GFP lines with the detailed amino acid sequences of the insertional junction regions.

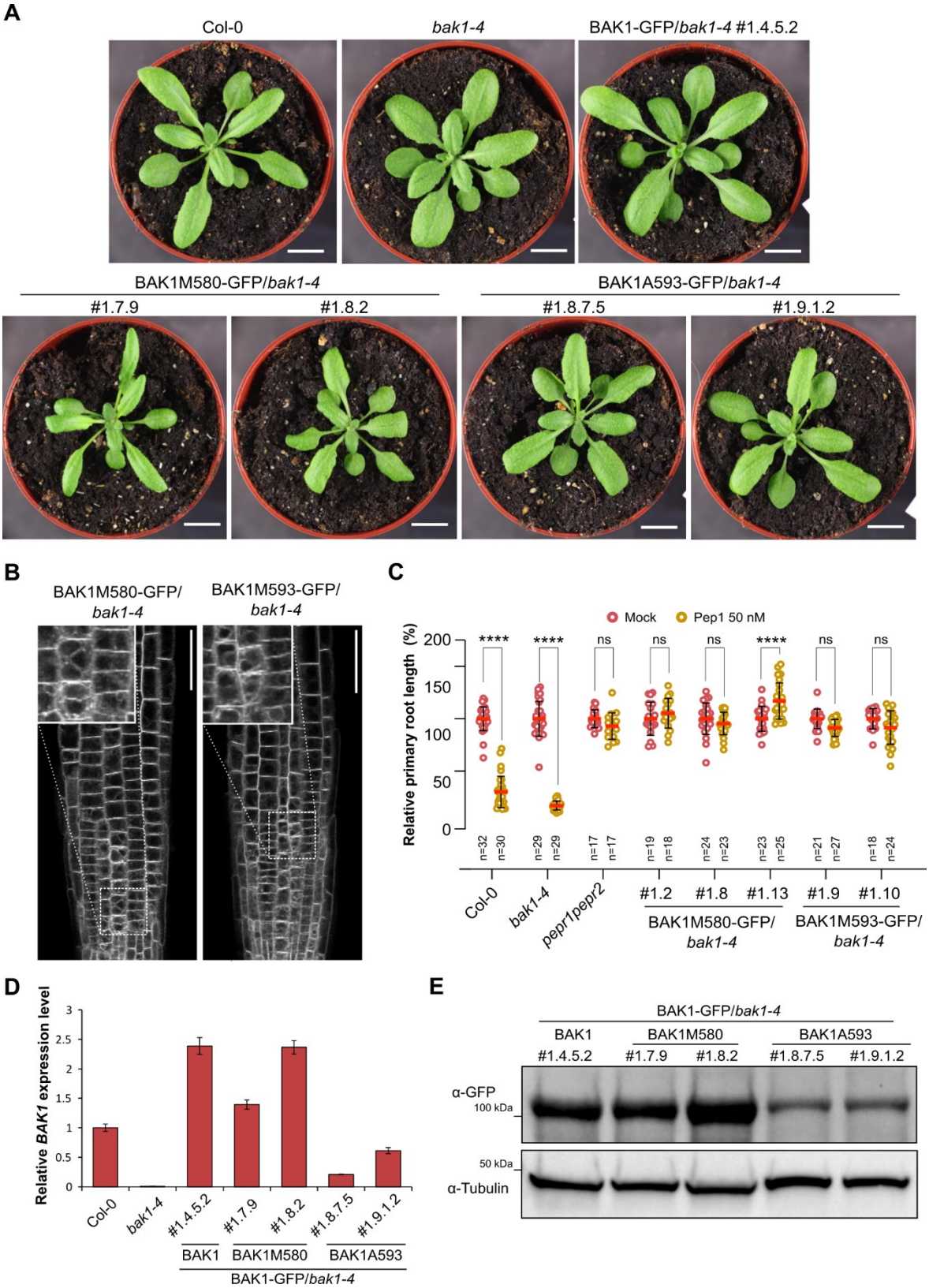

Supplemental Figure 9. GFP insertional mutagenesis screen for functional BAK1-GFP-expressing Arabidopsis lines.

(A) Representative images of 4-week-old T3 plants of the indicated genotypes. Scale bars, 1 cm.

1214 **(B)** Subcellular localization of BAK1-GFP in different GFP insertion lines. Root meristems of
1215 5-day-old seedlings were imaged. Scale bars, 10 µm.
1216 **(C)** Relative primary root length of seedlings of the indicated genotypes grown for 4 days on
1217 ½MS agar plates and transferred to ½MS solid media supplemented with 50 nM Pep1 or water
1218 (mock) for 3 days. Dots, red lines, and whiskers represent individual measurements, averages,
1219 and SD, respectively. The two-way ANOVA followed by Tukey's test was used to determine
1220 significant differences.****P<0.0001; ns, not significant; n, number of seedlings analyzed.
1221 (**D**) Real-time quantitative reverse transcription PCR (qRT-PCR) analysis of *BAK1*. Total RNA
1222 was isolated from 7-day-old seedlings of two independent transgenic lines. Transcript levels
1223 were normalized to *UBQ* gene with three technical replicates of each were quantified. Data are
1224 means ± SD
1225 (**E**) Total proteins isolated from 7-day-old seedlings and detected by Western Blotting (WB)
1226 with α-GFP antibodies to detect the BAK1-GFP. Numbers indicate individual transgenic lines.
1227 α-tubulin antibodies were used to equilibrate protein loading.
1228

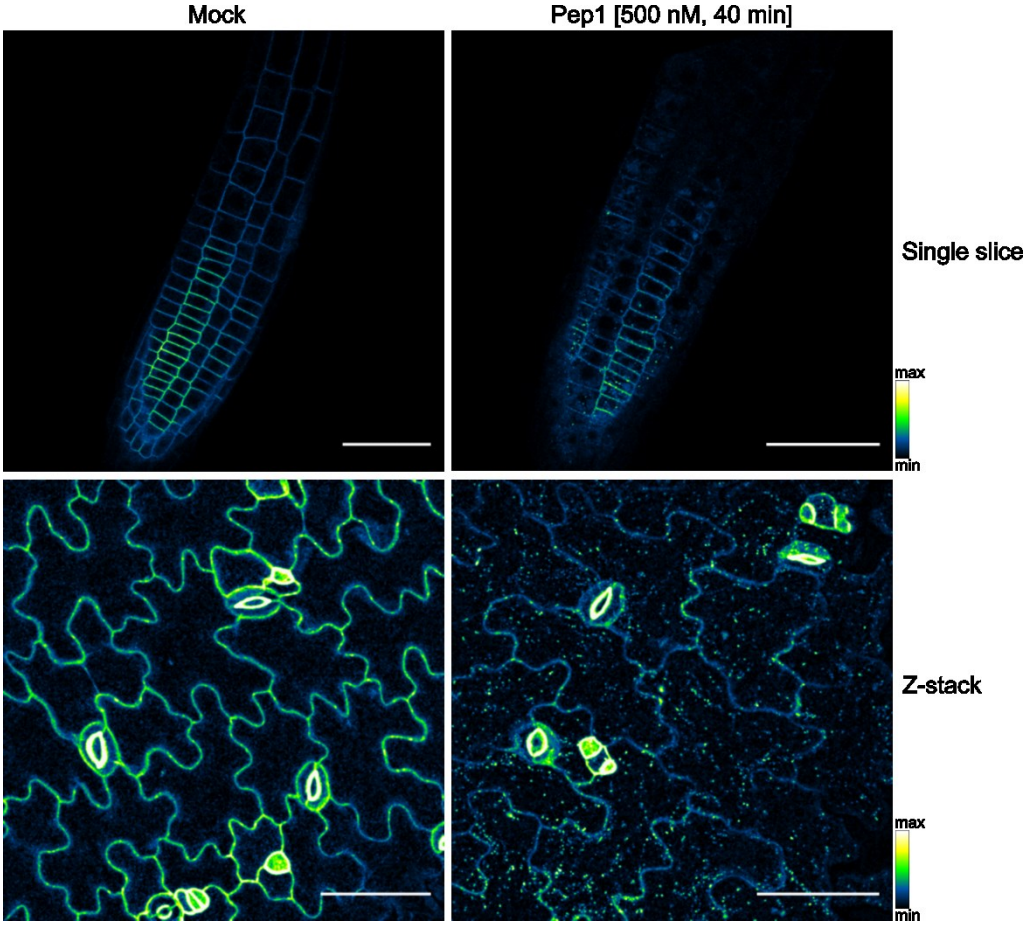

1229

1230

1231 **Supplemental Figure 10. PEPR1-GFP endocytosis in Arabidopsis root and shoot.**

1232 Representative images of PEPR1-GFP internalization visualized by color-based fluorescence
1233 intensity coding. Ten-day-old *pRPS5A-PEPR1-GFP*/*pepr1pepr2* seedlings were treated with
1234 water (mock) or 500 nM Pep1 for 40 min and root (top) and cotyledon (bottom) were imaged
1235 under confocal microscope. Images are maximum intensity Z-projections. Scale bars, 50 µm.

1236

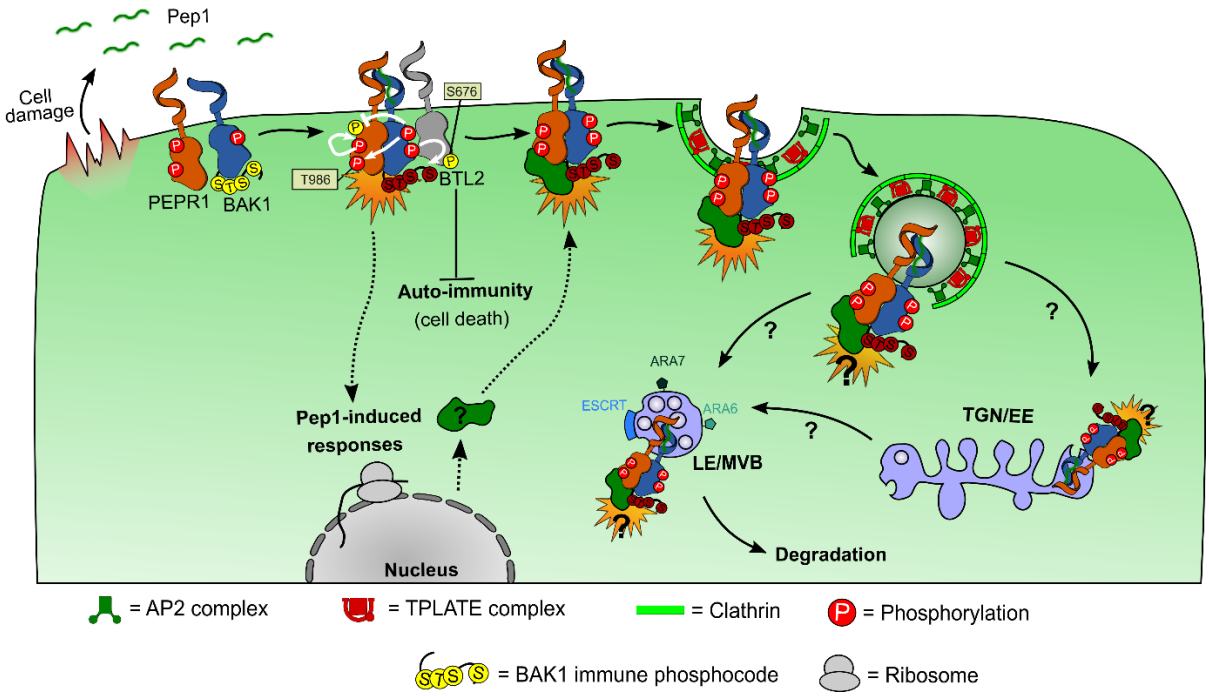

1237

1238 **Supplemental Figure 11. Proposed model of BAK1-PEPR1 activation and endocytosis.**
1239 Upon Pep1 perception, PEPR1 dimerizes with and trans-phosphorylates BAK1. This
1240 presumably triggers BAK1 phosphorylation at S602, T603, S604, and S612 residues, which are
1241 essential for Pep1-induced immune responses and PEPR1 endocytosis. Additionally, BAK1
1242 leads to an increase in PEPR1 phosphorylation, whereas PEPR1 eventually attenuates BAK1
1243 activity. Concurrently, BAK1 phosphorylates BAK-TO-LIFE 2 (BTL2) at S676, suppressing
1244 BTL2-mediated autoimmunity. PEPR1 is internalized together with BAK1 through clathrin-
1245 mediated endocytosis to eventually be degraded. This process might require the function of an
1246 unknown protein that is produced after the activation of the PEPR1-BAK1 complex by Pep1
1247 binding.

1248 **Supplemental Table 1. Primers used in this study**

1249

Name	Sequence (5'-3')	Application
UBQ10_Fw	GGCCTTGTATAATCCCTGATGAATAAG	qPCR
UBQ10_Rv	AAAGAGATAACAGGAACGGAAACATAGT	qPCR
GAPDH_Fw	TTGGTGACAACAGGTCAAGCA	qPCR
GAPDH_Rv	AAACTTGTCGCTCAATGCAATC	qPCR
mCtrine_Fw1	ATCATGGCCGACAAGCAGAA	qPCR
mCtrine_Rv1	TCTCGTTGGGGTCTTTGCTC	qPCR
BAK1_qPCR-Fw	GACAACCGCAGTGCGTGGGA	qPCR
BAK1_qPCR-Rv	TCGCGAGGCGAGCAAGATCA	qPCR
serk1-1-LP	ATACACAAAAGTGAAACGGCG	Genotyping
serk1-1-RP	TTAGACGAAGAATTCGAAGCG	Genotyping
serk2-1-LP	GGAAAACTCAGGTGATCCATTAAG	Genotyping
serk2-1-RP	TTAACAGGTGATGCACTGCAC	Genotyping
bak1-4-LP	CAGGGGCTATATGACCAATTG	Genotyping
bak1-4-RP	TCCTATCTCTCCTACACCGCC	Genotyping
serk4-1-LP	TGGCTCAGAAGAAAACCACAG	Genotyping
serk4-1-RP	CTGCTCCACTTCTGTTTCCAC	Genotyping
LBb1_3	ATTTTGCCGATTTCGGAAC	Genotyping
BAK1-Rv-K253	cctcgcccttgctcaccatAGATCCGCCGCCTCCAGAAGATCC GCCGCCTCCAGActtttttccttcgccaccaagct	Cloning
GFP-Fw-K253	agcttggtggcgaaggaaaaagTCTGGAGGCGGCGGATCTTCT GGAGGCGGCGGATCTatggtgagcaagggcgagg	Cloning
GFP-Rv-K253	acatcaaagaagtggtcctgcggTGAGCCTCCTCCGCCTGATGA GCCTCCTCCGCCTGActtgtacagctcgtccatgccg	Cloning
BAK1-Fw2-K253	cggcatggacgagctgtacaagTCAGGCGGAGGAGGCTCATCA GGCGGAGGAGGCTCAccgcaggaccacttctttgatgt	Cloning
BAK1-Attb2-Rv2-K253	TACCCAGCTTTCTTGTACAAAGTGGTCCCCttatcttggac ccgaggggtattc	Cloning
BAK1_Rv-K273	tcctcgcccttgctcaccatAGATCCGCCGCCTCCAGAttgtcctaaat gaacttctgggtcctc	Cloning
GFP_Fw-K273	gaggacccagaagttcatttaggacaaTCTGGAGGCGGCGGATCTa tggtgagcaagggcgagga	Cloning
GFP_Rv-K273	tagttcacgcaatgaaaacctcttcagTGAGCCTCCTCCGCCTGActt gtacagctcgtccatgccg	Cloning
BAK1_Fw2-K273	cggcatggacgagctgtacaagTCAGGCGGAGGAGGCTCActgaa gaggttttcattgcgtgaacta	Cloning

BAK1-Rv-M580	tcctcgcccttgctcaccatAGATCCGCCGCCTCCAGAcatttcctcct tttgccactcttcc	Cloning
GFP-Fw-M580	ggaagagtggcaaaaggaggaaatgTCTGGAGGCGGCGGATCTat ggtgagcaagggcgagga	Cloning
GFP-Rv-M580	ggttgggtagttgaaatcttgtctgaaTGAGCCTCCTCCGCCTGActt gtacagctcgtccatgccg	Cloning
BAK1-Fw2-M580	cggcatggacgagctgtacaagTCAGGCGGAGGAGGCTCAttcag acaagatttcaactacccaacc	Cloning
BAK1_Rv-A593	tcctcgcccttgctcaccatAGATCCGCCGCCTCCAGAggctggatg gtgggttggg	Cloning
GFP_Fw-A593	cccaacccaccatccagccTCTGGAGGCGGCGGATCTatggtgag caagggcgagga	Cloning
GFP_Rv-A593	cgccaatgatccagccagacacTGAGCCTCCTCCGCCTGActtgtac agctcgtccatgccg	Cloning
BAK1_Fw2-A593	cggcatggacgagctgtacaagTCAGGCGGAGGAGGCTCAgtgtc tggctggatcattggcg	Cloning
BAK1_Attb1	GGGGACAAGTTTGTACAAAAAAGCAGGCTATatggaa cgaagattaatgatcccttgc	Cloning
GFP_attB_Rv	TACCCAGCTTTCTTGTACAAAGTGGTCCCCttacttgtaca gctcgtccatgccg	Cloning
pOPINM_BAK1-Fw	AAGTTCTGTTTCAGGGCCCGCTTGGTGGCGAAGGA AA	Cloning
pOPINM_BAK1-Rv	ATGGTCTAGAAAGCTTTATCTTGGACCCGAGGGGT ATTC	Cloning
INM-BAK1-S612A-Rv	ATGGTCTAGAAAGCTTTATCTTGGACCCGCGGGGT ATTC	Cloning
INM-BAK1-AAA-Rv	ATGGTCTAGAAAGCTTTATCTTGGACCCGAGGGGT ATTCGTTTTCGATCTGGGCAGCGGCATCGCCAATGA TC	Cloning
PEPR1KDBAMHIFw	AAAAAGGATCCccTCTTTGTTGTTGAACAAAGTTCT TGCAG	Cloning
PEPR1KDECORI-Rv	TTTTTGAATTCTTACCGAACTGAATCAGAGGAGC	Cloning
PEPR1_Km-K855E_Fw	gaaaggtctacgctgtggagagacttgtattcgcg	Cloning
PEPR1_Km-K855E_Rv	cgcgaatacaagtctctccacagcgtagacctttc	Cloning
BIK1-Km_KK105AA_Fw	GTCATCGCCGTTGCAGCGCTTAACCAAGAA	Cloning
BIK1-Km_KK105AA_Rv	TTCTTGGTTAAGCGCTGCAACGGCGATGAC	Cloning
BAK1-Km_D416N-Rv	cagctttcacatTtcgatgaataatctttgg	Cloning
BAK1-Km_D416N-Fw	attattcatcgaAatgtgaaagctgcaaata	Cloning
BAK1-5_C408Y_Fw	ttacatgatcattAcgacccaaagattattcatc	Cloning

BAK1-5_C408Y_Rv	aatctttgggtcgTaatgatcatgtaaatac	Cloning
BIK1-AttB1-Fw	GGGGACAAGTTTGTACAAAAAAGCAGGCTCAATGG GTTCTTGCTTCAGTTCTCGA	Cloning
BIK1 _wo_stop-AttB2-Rv	GGGGACCACTTTGTACAAGAAAGCTGGGTACACAA GGTGCCTGCCAAAAGGTTT	Cloning

1250

1251